FACULTY OF INFORMATION TECHNOLOGY AND ELECTRICAL ENGINEERING

DEGREE PROGRAMME IN ELECTRONICS AND COMMUNICATIONS ENGINEERING
DEGREE PROGRAMME IN WIRELESS COMMUNICATIONS ENGINEERING

MASTER'S THESIS

High Reliability Downlink MU-MIMO with New Encoded OSTBC Approach and Superposition Modulated Side Information

Author	Nora Boulaioune
Supervisor	Prof. Nandana Rajatheva
Co-Supervisor	Prof. Matti Latva-aho
Second Examiner	Dr. Pekka Pirinen

March 2019

Boulaioune N. (2019) High Reliability Downlink MU-MIMO with New Encoded OSTBC Approach and Superposition Modulated Side Information. University of Oulu, Faculty of Information Technology and Electrical Engineering, Degree Programme in Wireless Communications Engineering. Master's Thesis, 54 p.

ABSTRACT

The promise of Fifth Generation Mobile Network (5G) heralded 5G-era with apparently unlimited potential outcomes. It resulted in the emergence of new paradigms of thought, better approaches to lead business, new innovative solutions, services and products, and is expected to transform the world as we know it. With the advent of some of those new technologies and use cases which deviate from the traditional human-centric, delay tolerant applications, the need for Ultra-Reliable Low-Latency Communications (URLLC) in the 5G wireless network has become indispensable.

In this thesis we investigate how to improve the reliability of a downlink multiuser (MU) MIMO transmission scheme with the use of a new approach of orthogonal space time block codes (OSTBC) and network coding with superposition modulated system and side information. The main advantage here is that we show multiple users can be accommodated with the same resource. This is quite useful in a wireless system where resources are always restricted. This therefore is a combination of two techniques to further enhance reliability. Orthogonality is useful in terms of resolving different signals from multiple antennas in a reduced complexity configuration. Superposition modulation with side information is important as it facilitates the recovery of symbols while still keeping the energy normalized. Thus we carried out a detailed analysis with the new OSTBC approach. It is shown that the performance of a multiuser (MU) MIMO system can be improved significantly in terms of bit, block and frame error rates (BER, BLER and FER) as reliability measures. By accommodating a reasonable number of multiple users, high reliability is achieved at the expense of bringing down the rate. To compensate for the low rate, conventional OSTBC is considered as well, where, as a penalty to pay, multiple orthogonal resources are required.

Keywords: 5G; high reliability; OSTBC; diversity; superposition modulation; network coding; receiver combining; downlink; MU-MIMO.

TABLE OF CONTENTS

FOREWORD

The focus of this thesis is to study a High Reliable Downlink MU-MIMO Scheme with a New Encoded OSTBC Approach and Superposition Modulated Side Information. This work was conducted at Centre for Wireless Communication (CWC) of University of Oulu as a part of High5 project. I was financially supported by Academy of Finland 6Genesis Flagship (grant no. 318927), Academy of Finland (Aka) (Grants no. 303532, no. 307492) and by the Finnish Funding Agency for Technology and Innovation (Tekes), Bittium Wireless, Keysight Technologies Finland, Kyynel, MediaTek Wireless, Nokia Solution and Networks.

First, I would like to show my deep gratitude to my principal supervisor, Prof. Nandana Rajatheva, whose most outstanding help in my research was to provide me with great insight into the research area. In addition, his caring attitude and his constant encouragement and inspiration helped to keep me on task throughout.

I would like to thank Prof. Matti Latva-aho for giving me the opportunity to join the research group in the CWC. I would never forget Dr. Pekka Pirinen, the project manager and the other colleagues at CWC for their support in my research.

Special thanks also go to my family, for their support and belief in me throughout all these years. They supported me in every step of my education and they have made lots of sacrifices for me to have a better future.

Lastly, my thanks to all those whose names I am unable to mention here but supported me in many respects during the completion of the thesis.

Oulu, Finland March 8, 2019

Nora Boulaioune

ABBREVIATIONS

Acronyms

2G	Second mobile Generation
3GPP	Third Generation Partnership Project
4G	Fourth mobile Generation
5G	Fifth Generation
AI	Artificial Intelligence
ARQ	Automatic Repeat-request
ASK	Amplitude Shift Keying
AWGN	Additive White Gaussian Noise
BEC	Backward Error Correction
BER	Bit Error Rate
BLER	Block-Error Rate
BS	Base Station
CSI	Channel State Information
DL	Downlink
EDGE	Enhanced Data for GSM Evolution
eMBB	Enhanced Mobile Broad-Band
FDD	Frequency Division Duplex
FEC	Forward Error Correction
FER	Frame Error Rate
FoF	Factories of Future
FSK	Frequency Shift Keying
GSM	Global System for Mobile communications
HARQ	Hybrid Automatic Repeat reQuest
ITU	International Telecommunications Union
LAN	Local Area Network
LEO	Low-Earth Orbit
LO	Local Oscillator
LSB	Least Significant Bit
LTE	Long Term Evolution
LTE-A	Long-Term Evolution Advanced
MCS	Multi-Cast Server
MIMO	Multiple Input Multiple Output
ML	Machine Learning
MU-MIMO	Multi-User Multiple Input Multiple Output
MSB	Most Significant Bit
MTC	Machine-Type Communications
mMTC	Massive Machine-Type Communications
NB-IoT	Narrow-Band Internet of Things
NC	Network Coding
NOMA	Non-Orthogonal Multiple Access
NR	New Radio
OFDM	Orthogonal Frequency-Division Multiplexing
OSTBC	Orthogonal Space-Time Block Codes

PDF	Probability Density Function
PSK	Phase Shift Keying
QAM	Quadrature Amplitude Modulation
RF	Radio Frequency
SIC	Successive Interference Cancellation
SNR	Signal to Noise Ratio
SPM	Super-Position Modulation
ST	Space-Time
STBC	Space-Time Block codes
TDD	Time Division Duplex
TTI	Transmission Time Interval
URLLC	Ultra-Reliable Low-Latency Communications
UE	User Equipment
UL	Uplink
W-CDMA	Wideband Code Division Multiple Access

Symbols

A	Amplitude
$A_{bb}(t)$	Amplitude of the baseband signal
$c_{SI-i,i+1}$	Side information coded sequence
D_1	First destination in the butterfly example
D_2	Second destination in the butterfly example
f	Frequency
$f_\alpha(\alpha)$	Probability density function of Rayleigh distribution
g_i^j	Convolutional encoder impulse response for output j
G_N	OSTBC matrix for the general case of N transmit antennas
G_2	OSTBC matrix for the case of 2 transmit antennas
G_4	OSTBC matrix for the case of 4 transmit antennas
$\mathbf{H}$	Channel matrix
$h_{n,m}$	Channel from transmit antenna n to receive antenna of user m
I	In-phase components of final modulated signal
$\mathbf{I}$	Identity matrix
K	Number of users and packets
M	Order of QAM (M-QAM)
$m_c^{(MSB)}$	Number of most significant bits of each symbol in SPM
$m_c^{(LSB)}$	Number of least significant bits of each symbol in SPM
$M(r/y')$	Viterbi k^{th} branch metric
$M^k(r/y')$	Viterbi k^{th} partial branch metric
N	Number of transmit antennas at the base station
P_1	First packet in the butterfly example
P_2	Second packet in the butterfly example
p_k	Packet of user k
$p_{SI-i,i+1}$	Side information packet
$P_{e,k}^{(i)}$	Probability of error in decoding packet p_i of user k
$P_{c,NC}^{(i)}$	Probability of correct recovery of p_i

Q	Quadrature components of final modulated signal
r	Viterbi received sequence
(r_1, r_2)	Superposition modulation weighting factor pair
$\mathcal{R}$	Physical resource
R	Rate of convolutional encoder
R_b	Modulation bit rate
R_s	Modulation symbol rate
S_1	First source in the butterfly example
s_2	Second source in the butterfly example
S_{RF}	Modulated RF signal to be transmitted
t	Time
u	Convolutional encoder input sequence
UE_k	User Equipment k
v	Codeword of convolutional encoder
$v_l^{(j)}$	Convolutional encoder sequence from output j
$\mathbf{X}$	STBC code matrix
$\mathbf{X}^H$	Complex conjugate transpose of $\mathbf{X}$
y'	Viterbi estimated sequence
α	Power split parameter in a superposition modulation
θ	Phase
ω	Angular frequency of the local oscillator
σ	Standard deviation
σ^2	Variance

Operators

$\lvert \cdot \rvert$	Absolute value
$\cos(x)$	Cosine function
$E\big[x\big]$	Expectation of a random variable x
$Im(x)$	Imaginary function
$\oplus$	Exclusive-OR
$Re(x)$	Real function
$Sgn(x)$	Sign function
$\sin(x)$	Sine function
$\sum$	Summation operation
$\prod$	Product operation

1. INTRODUCTION

This chapter initiates the thesis by describing the background and motivation about URLLC, thesis contribution which relates evaluation and purpose, followed by the wireless transmission scheme considered and assumptions made. At the end of the chapter a short overview of the content of the thesis is given.

1.1. Background and Motivation

Today, a substantial number of devices are connected, mobile phones connected to a mobile network and to the internet, just as computers connected to the internet. Now this connectivity has expanded into new devices, for example, tablets and smart watches. As E. Dahlman et al. states in [1], this is only the start of a completely connected society. The network raises various possibilities for new sorts of devices to connect in new places. These new kinds of gadgets can be household appliances, traffic control devices, sensors and significantly more. In addition, users of mobile phones and computers need higher data rate.

To enable this increase in data rate, access to communication in new areas, and diverse usage scenarios, a mobile network is being developed and standardized. This is called Fifth Generation, or 5G. Precisely what capabilities a 5G mobile network will have and what necessities a mobile network must satisfy so as be called 5G, is still being standardized. This procedure is carried out in standardization meetings, for example, the 3rd Generation Partnership Project (3GPP) and the International Telecommunications Union (ITU). The ITU produced a report called "Framework and overall objectives of the future development of IMT for 2020 and beyond" [2]. This report depicts the ITU's vision of the 5G society and is utilized as a structure to build up the prerequisites for 5G. In the report, the ITU recognized three usage scenarios to help various ranges of applications. These will be incorporated in the forthcoming 5G standard. The scenarios are:

1. **Massive Machine Type Communications (mMTC)**

   MTC manages the sort of communications in which machines communicate with each other autonomously without the need for human interference, likewise making possible the communication with and between machines by means of a mobile network [3]. Massive machine-type communication (mMTC) is a service classification to support the entrance of countless sort of machine-type devices [3]. With the expectation that MTC devices will follow an exponential growth, its advantages to the development of 5G innovation all around perceived. Moreover, the 3GPP has just started working on techniques to standardize MTC over cellular [4], [5]. Massive machine-type communications based services, such as sensing, tagging, metering, and monitoring, require high connection density and better energy efficiency [6]. Low power, wireless LAN systems, and capillary networks will supplement MTC connectivity [7].

   Throughout the years, there have been a few trials to support machine-type communications such as narrowband internet of things (NB-IoT) in licensed band, and SigFox and LoRa in unlicensed band [8]. These methodologies are similar

in spirit, but SigFox and LoRa technologies are suited for standalone services, while NB-IoT is a good fit for standards-compatible services. These approaches offer a few advantages, such as low power consumption, low operation cost, and improved coverage. However, in the scenario where devices significantly outnumber the resources used for the transmission, an aggressive connection strategy violating the orthogonal transmission principle is required. In recent years, approaches using non-orthogonal spreading sequence or user-specific interleaving have been proposed to suit a greater number of users than the traditional approach depending on orthogonal multiple access [6].

2. **Enhanced Mobile Broadband (eMBB)**

   Enhanced Mobile Broadband (eMBB) is a service category identified with high necessities for bandwidth, such as high-resolution video streaming, virtual reality, and augmented reality. The primary challenge in 4G systems is to enhance the system throughput (e.g., area, average, peak, perceived, and cell edge throughput). Physical layer technologies introduced to this end incorporate high order modulation transmission, carrier aggregation, cell densification via heterogeneous networks, and multiple-input multiple-output (MIMO) transmission. Basically, the principle objective of eMBB is in line with this direction. So as to accomplish 100-fold capacity increase over 4G systems, more aggressive physical layer technologies improving the spectral efficiency and exploiting the unexplored spectrum are required. Technologies under thought incorporate full-dimension and massive MIMO [9], millimeter-wave communication [10], and spectrally localized waveforms [11].

3. **Ultra-Reliable Low Latency Communication (URLLC)**

   Regardless of the enormous growth in the number of users, the commercial wireless technologies from 2G to 4G were not able to accomplish 99.999% reliability. This is on the grounds that the design of wireless communication technologies most of the time offer generally great connectivity with very low data rate in those territories where coverage is very poor with immoderate interference [12]. The communication stage where reliability is 99.999% ensured among devices and latency required is incredibly low is known as ultra-reliable low latency communication. URLLC is one of new operating modes in 5G that is making wireless a reliable commodity. URLLC from the point of view of supporting real-time applications with incredibly low latency requirement will be utilized in mission-critical communication (for instance drones, virtual reality, autonomous driving, remote surgeries) [13]. URLLC has mainly two functions, latency and reliability. Latency is the time a packet takes to arrive at the receiver's physical layer from transmitter's physical layer [14]. Reliability is the probability of successful data transmission within time period T. Reliability requests the successful data transmission under stringent latency requirements. Next, we inspect the basic empowering influences for high reliability and low-latency communication.

- **Low-Latency**

  Deterministic, arbitrary or random components influence latency. The minimum latency is characterized by deterministic components, with the latency's spread, mostly its tails, being influenced by the arbitrary or random components. The parts of deterministic latency incorporate the time-to-transmit data, the hold up time between transmissions information, and the overhead (reference signals, parity bits). While on the other hand, time-to-retransmit information, overhead (when required), queuing delay, random back-off times and other computing or processing delays, involve the arbitrary components [15]. In the following, we will examine the diverse types of empowering agents used for low latency communication:

1. **eMBB/URLLC multiplexing:** In light of its latency or reliability, a static or semi-static resource between eMBB and URLLC transmissions might be favored, however it is wasteful with regards to usage of resources, and thus requires dynamic multiplexing for proper operation [16]. Rather than improving power of resources that are narrow-band in nature, more frequency-domain resources can be appointed to a UL (uplink) transmission to achieve high system reliability for URLLC. It pursues that wide-ranging band resources will be required for URLLC uplink transmission, if increased reliability is to be achieved while keeping latency relatively low. Likewise, whenever any new low-latency packet arrives in the middle of a frame, the routinely scheduled traffic should be prevented, which can be achieved by using creative scheduling techniques. Simultaneously, for most extreme efficiency, the eMBB traffic should not be substantially influenced if URLLC outage capacity is increased [15].

2. **Short Transmission Time Interval (TTI), short frame structure and Hybrid Automatic Repeat reQuest (HARQ):** Its essential function is the reduction of TTI duration, which is accomplished by utilizing fewer OFDM symbols for each TTI and by restricting OFDM symbols through broader sub-carrier dispersing and by reducing the HARQ roundtrip-time. Similarly, when the OFDM symbol duration is decreased, the sub-carrier spacing increases. Therefore, the queuing impact is accentuated because of the availability of a fewer number of resource blocks in the frequency domain. In spite of this, control-overhead is expanded, resulting in reduced capacity due to lack of resources for other URLLC data transmissions, when TTI duration is clipped. This issue is effectively addressed by the use of grant-free transmission during the uplink. The downlink provides the capacity to deal with non-negligible queuing delays by utilizing longer TTIs at higher loads [16].

3. **On-device machine learning / Artificial intelligence (AI) on edge:** Machine Learning forms the basis for active and low-latency network systems. Conventionally the concept of ML is dependent upon only a single node (centralized). This single node has full access to a worldwide dataset and uses critical storage and computing capacity. Still, the inadequacies of this system for applications, which are delay sensitive and require high reliability, have warranted enthusiasm for distributed machine learning (e.g., Deep Learning and federated learning)

which is viewed the new avenue in the ubiquitous field of artificial intelligence, likewise called ML [17].

4. **Edge Caching, Computing and Slicing:** Studies have demonstrated that latency has been considerably reduced by edge computing resources and caching [18], [19]. With new innovation of resource-intensive-applications, these trends will proceed in future. Network slicing is another technology that is destined to stay in service for assigning committed resources (e.g., caching, bandwidth, computing) for services that are mission-critical.

5. **Grant-Free vs. Grant-Based Access:** It is either related to the dynamic scheduling of uplink (UL), or it might be related to intermittent traffic against periodic traffic with persistent scheduling. Devices operate on an optimum level when they are given fast access to uplink on a priority basis, yet this approach diminishes capacity since resources are already allocated. Similarly, semi-persistent, unutilized resources can be reallocated to eMBB traffic. For aggregate semipersistent scheduling, to reduce collisions, contention-based access is carried out, with similar characteristics and in a similar gathering. Here, a base station assumes a pivotal role in controlling the load and dynamically adjusting the resource pool. For ideal resource usage, the base set makes proactive scheduling of retransmission. It does this within the same group of UEs having a similar traffic [14].

6. **Joint Flexible Resource Allocation for UL/DL:** UL/DL operating simultaneously with time slot length versus switching cost is required for time division duplex (TDD) systems (study led in a context of LTE-A). LTE TDD and NR have been explored for frequency division duplex (FDD). While just NR have been examined for TDD since LTE TDD is not required for URLLC improvements [15].

7. **Low-Earth Orbit (LEO) satellites and unmanned aerial vehicles/systems:** Backhaul latency has been a major issue for long-range applications in rural regions. The use of low-earth orbiting satellites can perfectly resolve this issue. Additionally, the rising use of unmanned ariel systems can be of extraordinary help in reducing such latencies [15].

8. **Non-Orthogonal Multiple Access (NOMA):** NOMA decreases latency, since it supports more users that are sustained by orthogonal multiple access. It does as such by multiplexing the domain in the uplink and after that either utilizing successive interference cancellation (SIC) or different receivers which are further advanced, for example, message passing and turbo reception. In any case, issues such as user ordering, processing delay, imperfect channel state information, are not completely understood [20].

- **High Reliability**

  At the physical layer level, the reliability is influenced by channel, constellation, error detection codes, modulation techniques, diversity, and mechanisms of retransmission. Low rate codes to induce redundancy in poor channel conditions, retransmission to address errors and automatic repeat-reQuest (ARQ) in

transport layers, are a few methods used to increase reliability. Beamforming and diversity produce various free paths, which can be used from the transmitter to receiver and can likewise boost the signal-to-noise ratio. The basic difference between frequency diversity and time diversity is that the former occurs if the information is transmitted over a frequency-selective channel while the latter occurs when a forward error correction codeword is distributed on different channels. Multi-user diversity, happens when transmission relaying is done by using distinctive users directly from the source to the sink [15]. In the following lines, we shall discuss different tools that enhance reliability [15].

1. **Diversity via Network Coding and Relaying:** In circumstances where the phenomena such as diversity of time are unreliable and extreme fading of events happens, URLLC can only be guaranteed by dealing with factors such as diversity and sturdiness during the manufacturing stage. In this way, to ensure reliable, reciprocal communication without relying upon frequency and time diversity, it is appropriate to take full advantage of network coding (using concurrent relaying) and multi-user diversity. In a similar way, not only capacity is increased by increasing the density of the network, at the same time, latency is also diminished because of a decrease in the overall transmission range. Nonetheless, it comes at the expense of backhaul provisioning. Besides, spatial diversity by using multiple antennas is a practical solution in many cases that could be exploited as in [21].

2. **Multi-Connectivity and Harnessing Time/Frequency/RATs Diversity:** Time diversity is not generally a feasible solution, particularly in situations when the tolerable latency is smaller than channel coherence or in instances of stringent reliability requirements. As a general rule, three-dimensional diversity is used since frequency diversity is not always comparable to the number of users or devices. In this manner, highly reliable communication is best in enabling multi-connectivity.

3. **Data Replication (Contents and Computations):** Data replication is required whenever synchronization is not possible among nodes or at whatever point a backhaul with low-rate is required for synchronization, or whenever there is a lack of CSI. Nevertheless, this frequently reduces capacity. This failure can be avoided to continue replicating similar data over and over again except if an ACK is received in the occurrence of HARQ.

4. **Multicast:** Multicast is considerably more reliable when contrasted with unicast when it comes to receiving the same information. Reliability is dependent upon, the range of coverage and type of MCS used in the multicast group. The practicality of multicast is also reliant on factors such as the range of transmission (short or long) because cell edge users limit the performance.

5. **HARQ + Short Frame Structure, Short TTI:** This is used to accomplish high reliability. It does so by utilizing retransmissions to enhance outage capacity. Achieving the optimum level of MCS all the while remaining within the limits of reliability and latency constraints is an issue still open to look into.

1.2. Thesis Contribution

This Master's Thesis investigates how to improve the reliability of a downlink MU-MIMO transmission scheme, for this purpose, one would immediately think of applying different methods of diversity techniques.

The wireless system model consists of a base station equiped with N transmit antennas and attempts to communicate K equal size packets to single antenna receivers, our research objective is to combine side information with superposition modulation and thanks to a new encoded OSTBC approach multiple users are accommodated by sharing the same resource. Besides the diversity offered by STBC, the proposed design also exploits diversity through a novel strategy of constellation alignment based signal combining to enhance reliability of the side information transmission and compensate for the constrained power accessible in superposition modulation.

Scenarios are evaluated depending on the number of transmitting antennas at the base station and consequently the multiple users in the downlink. Simulation results for different scenarios are conducted and discussed in order to validate the error performance improvement of the proposed system.

1.3. Thesis Outline

The remaining of this thesis is organized as follows:

- **Chapter 2:** Consists of the necessary theoretical background and provides an overview of the main constitutional parts of the thesis.
- **Chapter 3:** Provides the details of the work carried out, where the general system model is described. Herein, details of the transmitter and receiver processing are visited, we provide detail derivations and analytical expressions related with the proposed system model.
- **Chapter 4:** Simulation results for different scenarios are considered and corroborated via Monte Carlo simulations. BER/BLER performance evaluations of the proposed system model are presented.
- **Chapter 5:** This chapter consists of a conclusion section which provides a summary to the thesis work and presents ideas for future work.

2. BACKGROUND AND LITERATURE

This chapter describes the theoretical background needed to understand the thesis. The main objective is to provide a sufficient background about the main blocks of a wireless communication system, where the focus is on the specific strategies considered for the system model introduced in this work. The work starts with the channel coding strategy and the decoding algorithm associated with it. Then it clarifies the modulation process in the transmitter and receiver, the strategies and assumptions related with this thesis work are presented as well.

2.1. Wireless Communication System

The basic elements of a wireless communication system are shown in Figure 2.1.

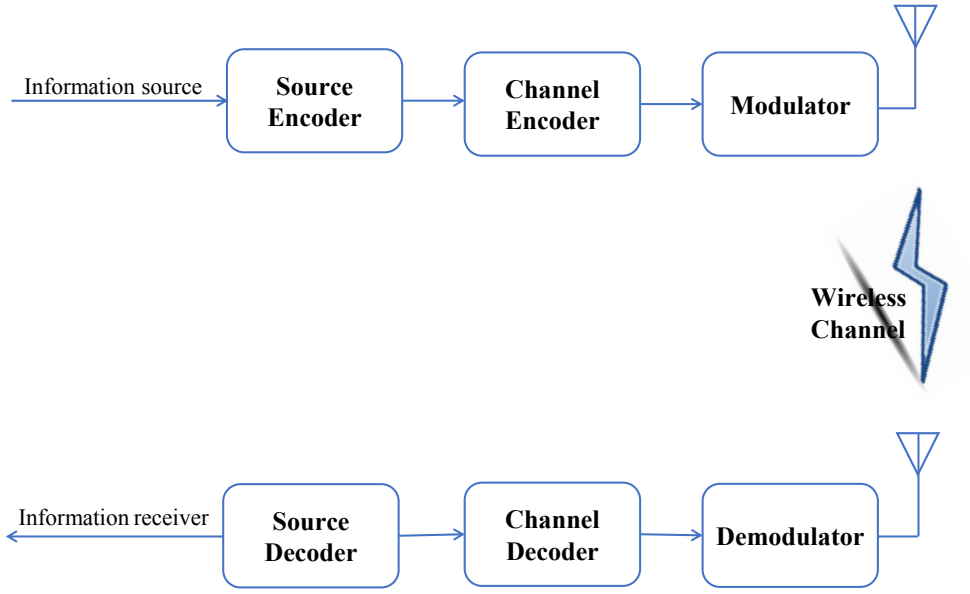

Figure 2.1. Block diagram of a wireless communication system.

Every communication system starts with a source of data that needs to be transmitted. The source encoder converts the input data, which could be either analog or digital, into a sequence of binary data. The binary data is passed through a channel encoder, which adds redundancy to the data. This is required to overcome the effects of noise added by the channel. Ratio of redundancy to data is dependent on the type of communication system. For a system having high level of noise, it would require more redundant information so as to help the receiver decode and correct the received data. There are different types of channel coding schemes, which are broadly classified into block codes, convolutional codes, and turbo codes. After adding up redundant data bits, the sequence of bits are mapped onto signal waveforms by the modulator block.

The receiver obtains the signal from antenna and samples it. At the receiver based on received sample and type of constellation, it is decided which symbol was transmitted by the transmitter. The symbol detected, which was encoded by the channel encoder,

is decoded by the channel decoder. As previously discussed, channel decoder detects, and corrects errors that are due to the channel. After successful decoding, source decoder converts the digital signal into a form that can be used by the user.

2.2. Channel Coding

The wireless communication channel causes impairments to the communications signal. These impairments are generally due to the inherent characteristics of different types of radio channels (noise, fading, and so on). The motivation behind channel coding is to make the transmission sufficiently strong against these channel impairments by adding redundancy to the transmitted signal [22]. Despite the fact that adding redundancy reduces the communication rate, channel coding is a fundamental part of each communication system since it makes communication more reliable.

There are two kinds of methodologies for channel coding [23]. The first is named forward error correction (FEC). This channel coding procedure recognizes errors and corrects them at the receiver side by misusing the redundancy in the transmitted signal. FEC approach does not require a feedback channel, thus it can be employed in latency critical systems. The second procedure is named as backward error correction (BEC) or automatic repeat-request (ARQ). In this channel coding system, the receiver detects the errors and demands a retransmission. Clearly, ARQ strategy requires a feedback channel, subsequently it may not be appropriate for latency-critical applications. However, it might be advantageous in bandwidth-critical systems.

2.2.1. Convolutional Codes

A convolutional code is a type of error-correcting code in which every m-bit information symbol to be encoded is transformed into an n-bit symbol, where m/n is the code rate ($n \geq m$) and the transformation is a function of the last k information symbols, where k is the constraint length of the code [24].

2.2.1.1. Encoding for Convolutional Codes

Convolutional codes are broadly used to encode digital data before transmission through noisy channels. The encoder has memory and the encoder outputs at any given time unit depend not just on the inputs at that time unit but also on some number of previous inputs. Information bits are divided into blocks with length k and these blocks are then mapped into the code words with length n. This operation is done independent of the length k.

Generator sequences are one approach to describe the encoder structure of convolutional codes. Generator sequences are acquired by applying impulses into the system. After getting the generator sequences, these sequences and input sequences are con-

volved to deliver the encoded sequences. All operations are modulo-2. Generator equation is

$$v_l^{(j)} = \sum_{i=0}^{m} u_{l-i} g_i^j = u_l g_0^j + u_{l-1} g_1^j + \cdots + u_{l-m} g_m^j, j \in \{0, 1, \dots\}. \tag{2.1}$$

In this manner, input sequences are encoded. Encoded information sequences are then multiplexed into a single sequence called a codeword for transmission over the channel. The codeword is given by

$$v = \left(v_0^{(0)} v_0^{(1)}, v_1^{(0)} v_1^{(1)}, v_2^{(0)} v_2^{(1)}, \dots\right). \tag{2.2}$$

Additionally, encoding can be written in a matrix form. Matrix form for encoding is:

$$v = uG. \tag{2.3}$$

Another encoding system of convolutional coding is by utilizing the state diagram. It contains memory elements whose content decides a mapping between the next set of input bits and output bits. Likewise, this state diagram is time-invariant. There are 2^k branches leaving each state in the state diagram and the states are appeared as $S_0, S_1, \dots, S_{2^{v-1}}$. State branches are shown as X/YY, where X is the input bit and YY is the output bits. Note that, the memory contents are the reverse of the binary representation of the state number. Example of state diagram is shown in Figure 2.2.

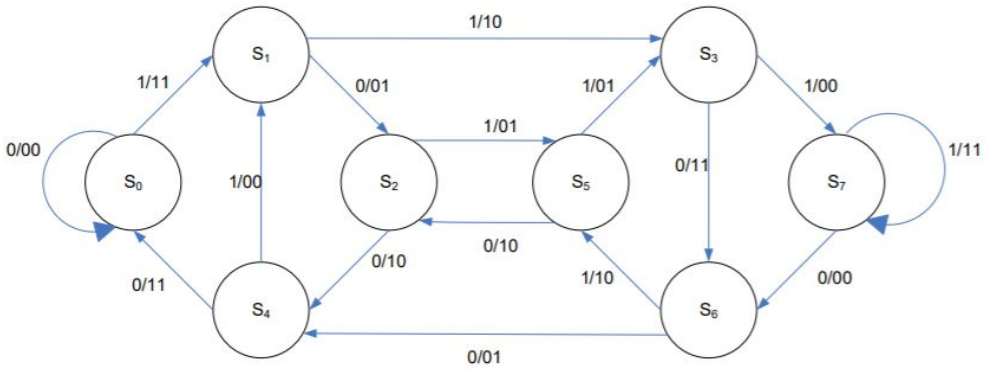

Figure 2.2. An example state diagram.

Consider that information sequence $u = (1011000)$ will be encoded with rate $R = 1/2$. Loop begins from S_0 and finishes S_0. Input bits will be checked looking at the state diagram. First bit of information sequence is 1. Looking at the state diagram with starting from S_0, output bits will be 11 and state will be S_1 . Next input bit is 0, then S_2 will be next state and the output bits will be 01. These operations proceed until the end of information sequence.

2.2.1.2. Convolutional Codes for Decoding

Viterbi algorithm is a fast operation for decoding convolutional codes. It demonstrates state diagram of the encoder in time and every time unit is represented with a separate state diagram. The subsequent structure of Viterbi is a trellis diagram.

2.2.1.3. Trellis Diagram

The trellis diagram is an expansion of a convolutional code's state diagram that explicitly demonstrates the passage of time. An example of trellis diagram will appear in Figure 2.4 for the encoder in Figure 2.3. Two neighboring states are connected by branches and trellis diagram branches are labeled with the output bits. These output bits are identified to the state transitions. Consider a general (n, k) binary convolutional encoder with total memory M and maximal memory order m. The associated trellis diagram has 2^M nodes at each stage or time increment t. There are 2^k branches leaving every node and one branch for each possible combination of input values. Additionally, there are 2^k branches entering to every node. Given an input sequence of kL (k is number of input and L is length of each input), the trellis diagram must have $L + m$ stages. The primary stage is starting and last stage is stopping. In addition to this, there are 2^{kL} distinct paths through the general trellis. Each one of these paths corresponds to a convolutional code word of length $n(L + m)$.

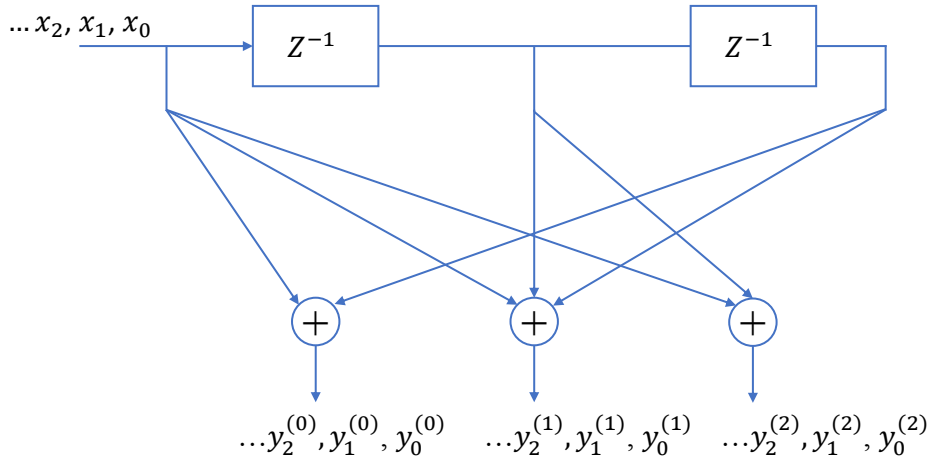

Figure 2.3. Encoder for a rate $R = 1/3$ convolutional code.

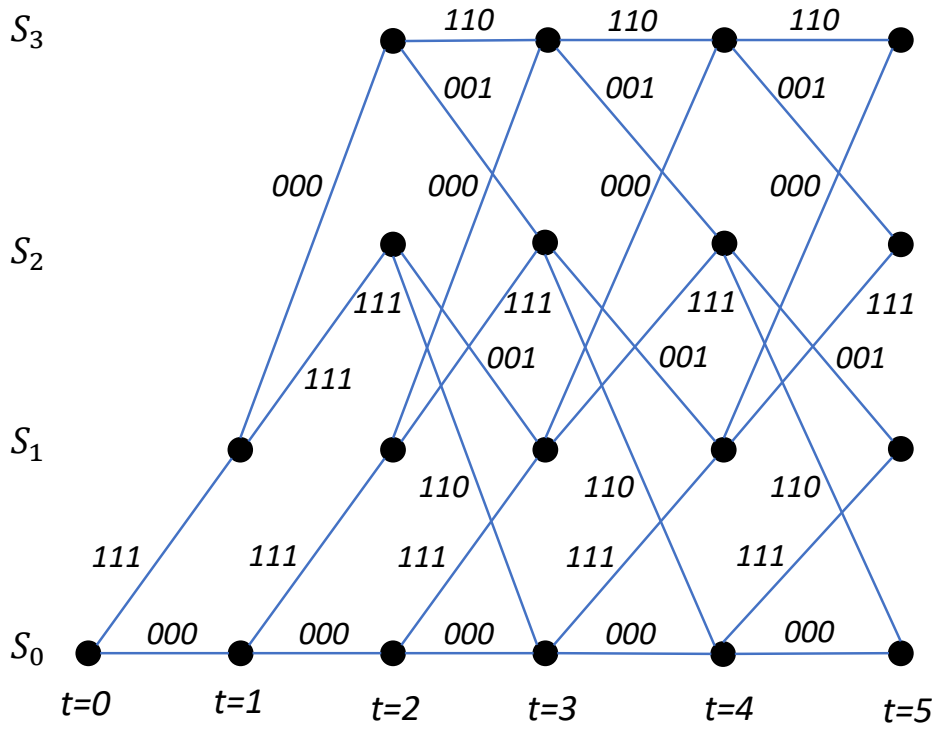

Figure 2.4. Trellis diagram for encoder in Figure 2.3.

2.2.1.4. Viterbi Algorithm

Information sequence is encoded and afterward transmitted and it is corrupted by noise. Received sequence is decoded with Viterbi in convolutional codes. The maximum likelihood decoder selects for estimate the transmitted sequence. This kind of decoder maximizes the probability of $p(r/y')$ in which, r is the received and y' is the estimated sequence.

Consider that, this information sequence x is made out of L k-bit blocks and this encoded code is named as y. At the end of encoding the output sequence comprises of L n-bit blocks. The number of blocks is expanded by m (long shift register) blocks. This sequence is transmitted and corrupted by noise. The received sequence is labeled as r. This sequence estimated y' by decoder and the decoder generates a maximum likelihood.

Formulas of x, y, r, y' are

$$x = \left(x_0^{(0)}, x_0^{(1)}, \ldots, x_0^{(k-1)}, x_1^{(0)}, x_1^{(1)}, \ldots, x_1^{(k-1)}, \ldots, x_{L-1}^{(k-1)}\right), \tag{2.4}$$

$$y = \left(y_0^{(0)}, y_0^{(1)}, \ldots, y_0^{(n-1)}, y_1^{(0)}, y_1^{(1)}, \ldots, y_1^{(n-1)}, \ldots, y_{L+m-1}^{(n-1)}\right), \tag{2.5}$$

$$r = \left(r_0^{(0)}, r_0^{(1)}, \ldots, r_0^{(n-1)}, r_1^{(0)}, r_1^{(1)}, \ldots, r_1^{(n-1)}, \ldots, r_{L+m-1}^{(n-1)}\right), \tag{2.6}$$

$$y' = \left(y'^{(0)}_0, y'^{(1)}_0, \ldots, y'^{(n-1)}_0, y'^{(0)}_1, y'^{(1)}_1, \ldots, y'^{(n-1)}_1, \ldots, y'^{(n-1)}_{L+m-1}\right). \tag{2.7}$$

Path metric equation is

$$M(r/y') = \sum_{i=0}^{L+m-1} \big(\sum_{j=0}^{n-1} M\big(r_i^{(j)}/y'^{(j)}_i\big)\big). \tag{2.8}$$

The k^{th} branch metric is the sum of the bit metrics for the k^{th} block of r given y'

$$M(r/y') = \sum_{j=0}^{n-1} M\big(r_k^{(j)}/y'^{(j)}_k\big). \tag{2.9}$$

The k^{th} partial branch metric is sum of the branch metrics for the first k branches

$$M^k(r/y') = \sum_{i=0}^{k-1} \big(\sum_{j=0}^{n-1} M\big(r_i^{(j)}/y'^{(j)}_i\big)\big). \tag{2.10}$$

Trellis diagram is used for calculation of path metrics in Viterbi algorithm. Every node in the trellis is assigned a number and these numbers are the partial path metric of the path. This path begins from state S_0 at time $t = 0$ and finishes at that node and best partial path metric is chosen among all entering paths.

2.3. Modulation

For any application of wireless communication a specific channel is defined. Wireless channels as usual have limitations. For instance, carrier frequency ought to be in a special range. Such limitations can be overcome by signal modulation. In modulation process baseband data is up converted to a higher frequency and afterward transmitted to the channel through antenna. In the receiver side, the received signal should be down converted so as to generate the baseband data. The modulator does the task of modulating local oscillator (LO) signal with baseband data and, at the receiver side the demodulator does the inverse of this procedure to recover the baseband data.

A pure sinusoidal signal in time domain can be distinguished by its three main characteristics which are frequency (f), phase (θ) and amplitude (A):

$$A \sin\big(2\pi f t + \theta\big). \tag{2.11}$$

These three characteristics can be utilized to transmit data [25]. Consequently, modulation is achieved in three ways: loading information either on changing amplitude, frequency and phase or a combination of these. Digital modulation is achieved by mapping bits onto finite levels of any of these dimensions. The type of digital modulation schemes can be summarized as follows.

- Amplitude Shift Keying (ASK): bits are mapped onto finite set of amplitude levels. The number of levels depends on how many bits are mapped.
- Frequency Shift Keying (FSK): in this modulation type, there are finite sets of frequency levels.
- Phase Shift Keying (PSK): there are finite levels of phases on which bits are mapped.

2.3.1. Amplitude Modulation

In this modulation technique, baseband data modulates the LO signal by changing its amplitude. This can effectively be possible by multiplying the baseband data by LO signal. Thus, the peak of the modulated signal is the same as the baseband signal. In the demodulator, the peak of the modulated signal can be obtained using simple low-pass filter

$$S_{RF} = A_{bb}(t)\cos\big(\omega t\big), \tag{2.12}$$

where S_{RF} is the modulated signal to be transmitted (RF signal), $A_{bb}(t)$ is the amplitude of the baseband signal and ω is the angular frequency of the local oscillator, $\omega = 2\pi f$.

In digital communication, data is first transformed to binary form, i.e., the baseband data amplitude can just take values 0 and 1. The baseband data is first applied to a serial to parallel converter to produce two set of data $\big(X_I$ and $X_Q\big)$ with half data rate. These two sets of data modulate two orthogonal signals having a similar carrier frequency to generate in-phase $\big(I\big)$ and quadrature $\big(Q\big)$ components of final modulated signal. I- and Q-signals are added to form the final modulated signal (Figure 2.5). This is named as quadrature amplitude modulation (QAM) [26].

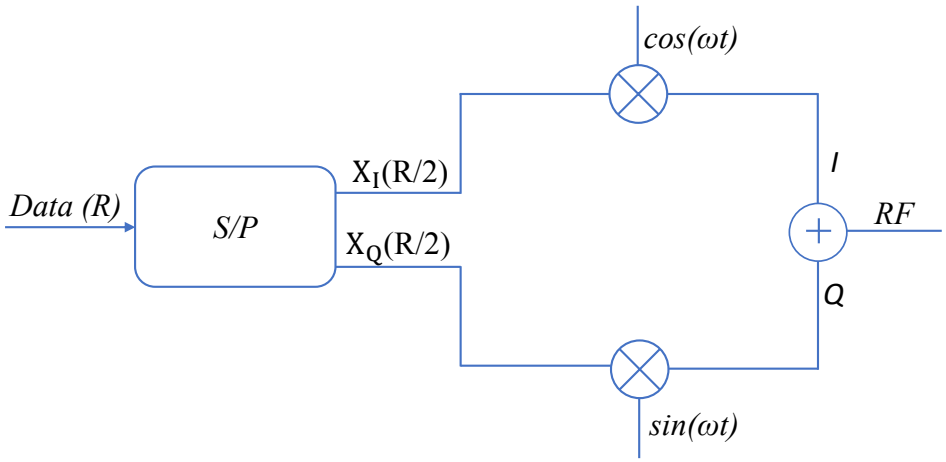

Figure 2.5. QAM modulation scheme.

The final modulated signal (RF signal) as the sum of I- and Q-components is mathematically expressed as:

$$S_{RF} = X_I\cos\big(\omega t\big) + X_Q\sin\big(\omega t\big), \tag{2.13}$$

where S_{RF} is the RF signal, and ω is the angular frequency of the local oscillator. The simplest M-QAM modulation scheme is QAM. In QAM, X_I and X_Q can just take two values of -1 and 1. In total, $2^2 = 4$ symbols can be introduced in QAM, each symbol containing two bits. These symbols are shown in Figure 2.6.

It is also possible to take every n bit of data as a symbol, at that point there are absolutely 2^n symbols and the modulation is called 2^n-QAM. For this situation, each

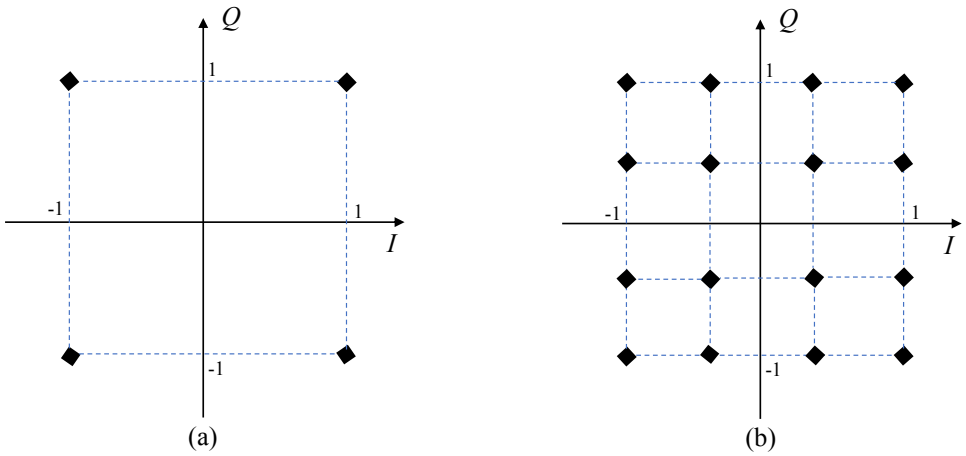

Figure 2.6. (a) QAM modulation symbols, (b) 16-QAM modulation symbols.

of X_I and X_Q components should represent $n/2$ bits in a symbol and take $2^{n/2}$ amplitude levels. For instance, in 16-QAM modulation, there are totally 16 symbols, n is $log_2(16) = 4$, i.e., each 4 bit form one symbol, X_I and X_Q take $2^2 = 4$ amplitude levels. 16-QAM modulation symbols appear in Figure 2.6b. It is evident now that in 2^n-QAM modulation each symbol corresponds to n bits. The relation between bit rate and symbol rate is expressed as

$$R_b = nR_s, \tag{2.14}$$

where R_b is bit rate and R_s is symbol rate. For QAM modulation n is 2.

Finally, quadrature amplitude modulation (QAM) is generated by changing both the phase and amplitude of the signal. The bits are mapped to two analogue signals by changing the amplitude and phase. The two analogue signals (sinusoids) are out of phase with each other by $90°$, making them orthogonal. The modulated signals are summed up and the resulting waveform is the combination of both PSK and ASK.

2.3.2. Superposition Modulation

A superposition modulation can be obtained by appropriately combining of two uniform constellations. Figure 2.7 demonstrates the generation of the super-symbols resulting from superimposing two 4-QAM constellations. It can be seen that the constellation map of the super-symbol is similar to that of a 16-QAM scheme. A superposition modulation weighting factor pair (r_1, r_2) is defined, where r_1 is assigned to x_1, while r_2 is assigned to x_2, x_1 and x_2 are the constituent complex symbols. Then the superposition modulation symbol can be expressed as [27]

$$x = r_1 x_1 + r_2 x_2, \tag{2.15}$$

where $E\left[|x_1|^2\right] = 1$ and $E\left[|x_2|^2\right] = 1$, since the average symbol power is thought to be unity. At the point, when the two 4-QAM symbols are multiplied using their SPM weighting factors, their average power can be denoted as

$$E\left[|r_1\mathbf{x}_1|^2\right] = r_1^2 E\left[|\mathbf{x}_1|^2\right] = r_1^2, \tag{2.16}$$

$$E\left[|r_2\mathbf{x}_2|^2\right] = r_2^2 E\left[|\mathbf{x}_2|^2\right] = r_2^2. \tag{2.17}$$

Considering that the average symbol power of the super-symbol ought to be also unity, we have

$$\begin{aligned} E\left[|\mathbf{x}|^2\right] &= E\left[|r_1\mathbf{x}_1 + r_2\mathbf{x}_2|^2\right] \\ &= E\left[r_1^2\mathbf{x}_1^2 + r_2^2\mathbf{x}_2^2 + 2r_1r_2\mathbf{x}_1\mathbf{x}_2\right] \\ &= r_1^2 E\left[|\mathbf{x}_1|^2\right] + r_2^2 E\left[|\mathbf{x}_2|^2\right] + 2r_1r_2 E\left[\mathbf{x}_1\mathbf{x}_2\right] \\ &= r_1^2 + r_2^2 + 2r_1r_2 E\left[\mathbf{x}_1\mathbf{x}_2\right] \\ &= 1. \end{aligned} \tag{2.18}$$

Moreover, the two 4-QAM symbol streams are independent of each other, yielding

$$E\left[\mathbf{x}_1\mathbf{x}_2\right] = E\left[\mathbf{x}_1\right]E\left[\mathbf{x}_2\right] = 0, \tag{2.19}$$

where$E\left[\mathbf{x}_1\right] = E\left[\mathbf{x}_2\right] = 0$. Thus, the SPM weighting factor pair should fulfill

$$r_1^2 + r_2^2 = 1. \tag{2.20}$$

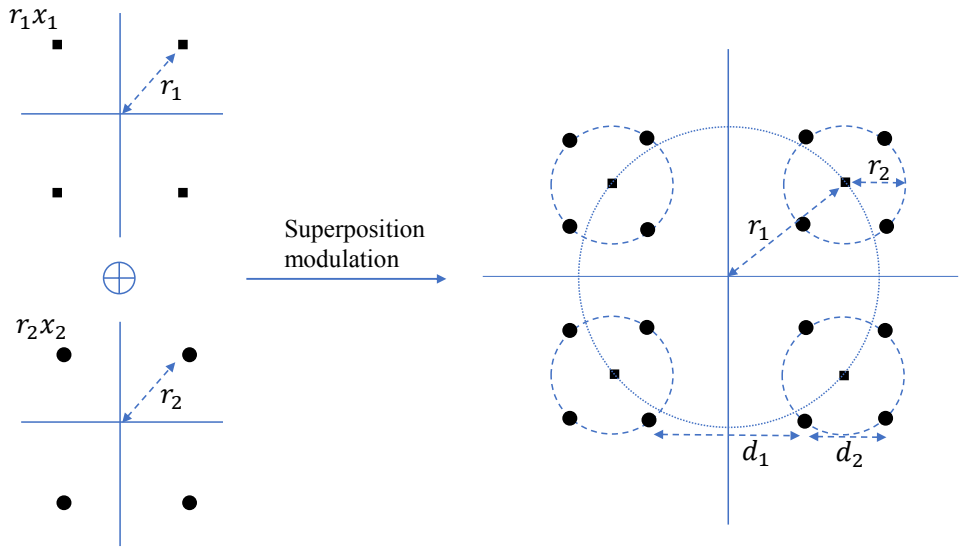

Figure 2.7. The generation of a 16-QAM super-symbols set from two 4-QAM symbol sets.

It might be seen from Figure 2.7 that in case the factor r_1 is larger than r_2, the constellation map of the super-symbol would be the extension of the constellation map

of x_2 based on the constellation map of x_1. Here we determine x_1 to be the dominant symbol and x_2 to be the auxiliary symbol.

Normally, a higher minimal Euclidean distance in a constellation set entails having a higher resistance against channel fading and noise. Note that a super-symbol is the combination of the dominant symbol and the auxiliary symbol, where the dominant symbol has a larger minimal Euclidean distance, thus exhibiting in an enhanced BER performance contrasted with that of the auxiliary symbol.

2.4. Network Coding

Network coding is considered to be discussed the first time in a seminal paper by Ahlswede *e*t al. [28]. They presented the possibility of a single node in the network combining incoming packets using linear combinations of these packets. The advantages of network coding are to be able to enhance throughput, robustness, complexity and security [29].

The most ideal way how to demonstrate the principle of network coding is through the well known butterfly example as appeared in Figure 2.8.

The scenario in Figure 2.8 can be described along these lines. Source S_1 needs to convey packet $P_1$to both destinations D_1 and D_2 just as source S_2 needs to send packet P_2 to the same pair of receivers. For this example we assume that all links have a capacity of one packet per second. In the event that routers R_1 and R_2 just store and forward the packets they receive, the middle link be overwhelmed because both routers consistently can either deliver P_1 to D_2 or P_2 to D_1 but not the two variants. Compare this and the circumstance where the router feeding the middle link with XORs (XOR operation is denoted by $\oplus$) of the two packets from the sources and sends $P_1 \oplus P_2$, as it appears in Figure 2.8. In that case both receivers can acquire both packets. Destination D_1 can get P_2 by XORing packet P_1 received on the direct link from S_1 with broadcasted $P_1 \oplus P_2$ from the router R_2. And analogically D_2 recuperates packet from source S_1 [30].

This arrangement is optimal in the sense of the maximal throughput, and for this situation the final throughput is two packets per channel usage. This approach is simply superior to the routing approach which can, at the best possible scenario, achieve 1.5 packet throughput per channel usage.

2.5. Space-Time Block Codes

Space time block coding (STBC) is the strategy of transmitting information with the help of multiple antenna system and exploiting the received information so as to improve the reliability of the transmitted information in a cellular and wireless environment. The principal objective of STBC is to convey the most suitable output and subsequently achieving maximum diversity gain. The transmitted signal gets scattered, reflected, and refracted before it reaches the receiver, and further this signal gets corrupted by the thermal noise of the receiver. This increases the probability of receiving some signals that are better than others. At the same time the possibility of acquiring the true signal after decoding the received signal gets better. STBC plays an essential

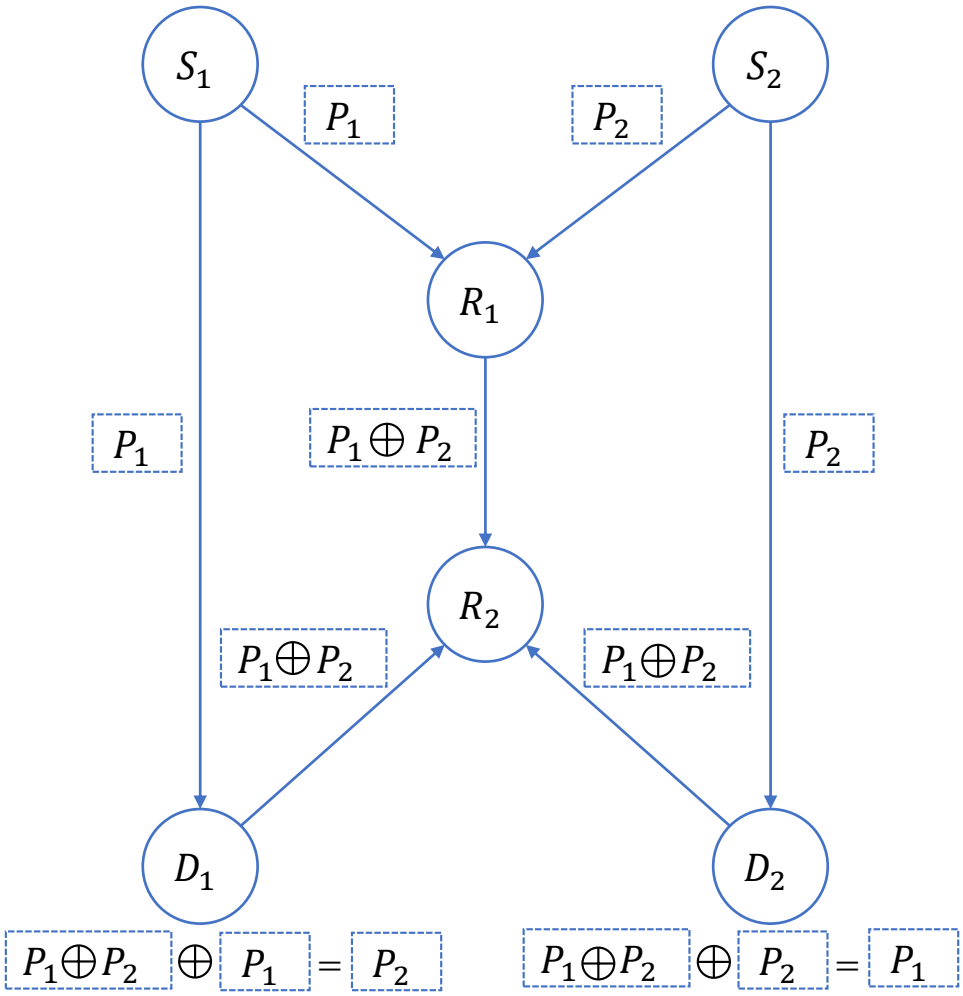

Figure 2.8. Network coding butterfly scenario example.

role in this, it combines all the received signals in an ideal and optimal way and aides in extracting all the possible information from the signal. In STBC the data is transmitted in a stream of encoded blocks, which is distributed over space and time. It is compulsory to have multiple transmit antennas, while it is not important to have multiple array of receiving antennas. However, it is seen that the performance of the system enhances with multiple receiving antennas [31], [32]. This process of receiving duplicates of the transmitted information through different channels is known as diversity reception.

2.5.1. Orthogonality

STBC is fundamentally an orthogonal system. This implies the vectors of the STBC networks are structured in such a design, that the vectors of the coding matrix are orthogonal at any given time and space. This yields a basic, optimal, and linear decoding at the receiving terminal. The only disadvantage of the orthogonal system is that any

one of the received signal that fulfills the above criterion has to sacrifice some portion of its data rate.

2.5.2. Orthogonal Space Time Block Code

Orthogonal space time block codes (OSTBC) fall under the linear STBC class of block coding. A linear STBC could be characterized as a code matrix whose real and imaginary parts are linear [33]. The generalized mathematical representation of OSTBC is given as

$$\mathbf{X} = \sum_{i=1}^{N} \left[Re\{x_i\}\mathbf{A}_i + jIm\{x_i\}\mathbf{B}_i \right], \tag{2.21}$$

where $\mathbf{A}_i$ and $\mathbf{B}_i \in \mathbf{C}^{i_t \times R}$, and are termed as covariance matrices.

OSTBC is most remarkably known for having simple maximum likelihood (ML) detectors that decouple distinctive symbols s_i, and subsequently accomplishing full diversity gain of order equal to $n_r \times n_t$. OSTBCs, due to their low decoding complexity are the premium choice for the most complex receivers. The principal objective of OSTBC design is to reach the optimum diversity gain. Hence, OSTBCs offer smaller coding gains compared with other ST codes. The main downside of OSTBC is that the bandwidth efficiency is compromised (lost), when the number of transmit antennas is more than two. For a source with two transmit antennas (Alamouti scheme), OSTBC is being considered as one of the most suitable means for enhancing the overall performance of the wireless communication systems. Furthermore, for the enhanced data rates for GSM evolution (EDGE), Alamouti code which is a 2×2 OSTBC, has been adopted as the standard in the 3rd generation cellular W-CDMA systems.

OSTBC has got its name in view of a specific unitary property, i.e.,

$$\mathbf{X}\mathbf{X}^H = \sum_{i=1}^{i_s} |s_i|^2 \, \mathbf{I}, \tag{2.22}$$

where s_i is the i^{th} symbol of the data matrix, $\mathbf{I}$ represents the identity matrix, $\mathbf{X}^H$ is the Hermitian matrix, $\mathbf{X}$ is the unitary matrix and i_s is the number of the symbols.

OSTBC was first presented and derived in [34], the well known study on the error performance using the unitary matrix $\mathbf{X}$. OSTBCs, that depend on amicable orthogonal designs have simple receiver structure and henceforth have minimum processing at the receiver [35]. If there is a complex constellation, OSTBCs are the most appropriate because of their amicable orthogonality. Orthogonal codes that are designed using amicable orthogonal designs are more likely to achieve full code rate of unity with a two transmit antenna system.

In order to understand the idea of code matrices $\mathbf{X}$ being proportional to the unitary matrices, and how the detection of symbols s_i are decoupled is ensured. Let us understand the concept of ML matrix for symbol detection. If the unitary matrix $\mathbf{X}$ fulfills (2.24), at that point

$$\begin{aligned}
\|\mathbf{Z}-\mathbf{HX}\|^2 &= \|\mathbf{Z}\|^2 - 2ReTr\{\mathbf{Z}^H\mathbf{HX}\} + \|\mathbf{HX}\|^2 \\
&= \|\mathbf{Z}\|^2 - 2\sum_{i=1}^{i_s} ReTr\{\mathbf{Z}^H\mathbf{HA}_i\}\bar{s_i} 2\sum_{i=1}^{i_s} ImTr\{\mathbf{Z}^H\mathbf{HB}_i\}\tilde{s_i} + \|\mathbf{H}\|^2 \cdot \|s\|^2 \\
&= \sum_{i=1}^{i_s} \big(-2ReTr\{\mathbf{Z}^H\mathbf{HA}_i\}\bar{s_i} + 2ImTr\{\mathbf{Z}^H\mathbf{HB}_i\}\tilde{s_i} + \left|s_i^2\right| \|\mathbf{H}\|^2 \big) + const\cdot \\
&= \|\mathbf{H}\|^2 \cdot \sum_{i=1}^{i_s} \left| s_i - \frac{ReTr\{\mathbf{Z}^H\mathbf{HA}_i\} - iImTr\{\mathbf{Z}^H\mathbf{HB}_i\}}{\|\mathbf{H}\|^2} \right|^2 + const\cdot
\end{aligned} \tag{2.23}$$

Moreover, the relation between amicable orthogonal designs and OSTBC is given by

$$\mathbf{XX}^H = \sum_{i=1}^{i_s} |s_i|^2 \mathbf{I}, \tag{2.24}$$

where $\mathbf{XX}^H$ stands for all complex s_i if and only if $\mathbf{A}_i$, $\mathbf{B}_i$ are of amicable orthogonal designs, i.e.,

$$\begin{aligned}
&\mathbf{A}_i\mathbf{A}_i^H = \mathbf{I}, \mathbf{B}_i\mathbf{B}_i^H = \mathbf{I} \\
&\mathbf{A}_i\mathbf{A}_q^H = -\mathbf{A}_q\mathbf{A}_i^H, \mathbf{B}_i\mathbf{B}_q^H = -\mathbf{B}_q\mathbf{B}_i^H, i \neq q \\
&\mathbf{A}_i\mathbf{B}_q^H = \mathbf{B}_q\mathbf{A}_n^H, for\ i = 1, \ldots, i_s, q = 1, \ldots, i_s\cdot
\end{aligned} \tag{2.25}$$

2.5.3. Alamouti Code

The very first and well-known STBC is the Alamouti code, which is a complex OSTBC specialized for the case of two transmit antennas. Figure 2.9 illustrates the Alamouti encoder. Firstly, the bit streams are modulated by using a M-ary modulation format. Then, the Alamouti encoder takes a block of two modulated symbols x_1 and x_2 in each encoding operation and gives it to the transmit antennas according to the code matrix [36]

$$\mathbf{X} = \begin{pmatrix} x_1^2 & x_2^2 \\ -x_2^* & x_1^* \end{pmatrix}. \tag{2.26}$$

As depicted in Figure 2.9, Alamouti encoded signal is transmitted from the two transmit antennas over two successive time slots. During the first time slot, two different symbols x_1 and x_2 are simultaneously transmitted from the two transmit antennas. During the second time slot, these symbols are transmitted again, where $-x_2^*$ is transmitted from the first transmit antenna and x_1^* is transmitted from the second transmit antenna.

Note that the Alamouti codeword $\mathbf{X}$ described above is a complex-orthogonal matrix, that is

$$\mathbf{X} = \begin{pmatrix} |x_1|^2 + \left|x^2\right|^2 & 0 \\ 0 & |x_1|^2 + \left|x^2\right|^2 \end{pmatrix} = \big(|x_1|^2 + |x_2|^2\big)\mathbf{I}_2. \tag{2.27}$$

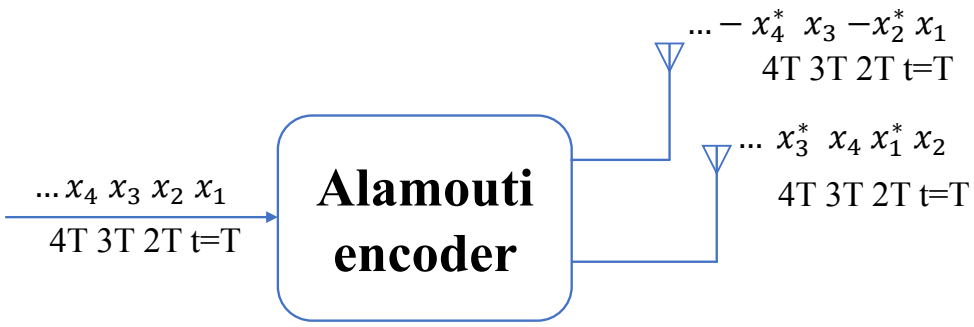

Figure 2.9. Structure of Alamouti encoder.

2.5.3.1. Detection Method

Herein, we discuss about the ML signal detection for Alamouti code. Assuming one receive antenna at the receive end and channel matrix $\mathbf{H} = [h_{ij}]$, $i = 1$, $j = 2$. The received signal can be presented as [36]

$$\begin{aligned} r_1^{(1)} &= r_1(t) = h_{11}x_1 + h_{12}x_2 + n_1^{(1)} \\ r_1^{(2)} &= r_1(t+T) = -h_{11}x_2^* + h_{12}x_1^* + n_1^{(2)}, \end{aligned} \tag{2.28}$$

where r_1 is the received signal at antenna 1, h_{ij} is the channel from the j^{th} transmit antenna and the i^{th} receive antenna, n_1 is a complex random variable representing noise at antenna 1, and $s_{(k)}$ denotes s at time instant k.

Before the received signals are sent to the decoder, they are combined as follows [36]

$$\begin{aligned} \tilde{x}_1 &= h_{11}^* r_1^{(1)} + h_{12} r_1^{*(2)} \\ \tilde{x}_2 &= h_{12}^* r_1^{(1)} + h_{11} r_1^{*(2)}. \end{aligned} \tag{2.29}$$

Substituting (2.28) in (2.29) yields

$$\begin{aligned} \tilde{x}_1 &= \left(\alpha_{11}^2 + \alpha_{12}^2\right)x_1 + h_{11}^* n_1^{(1)} + h_{12}^* n_1^{(2)} \\ \tilde{x}_2 &= \left(\alpha_{11}^2 + \alpha_{12}^2\right)x_2 - h_{11}^* n_1^{(2)} + h_{12}^* n_1^{(1)}, \end{aligned} \tag{2.30}$$

where α_{ij}^2 is the square of the channel h_{ij}. The calculated $\tilde{x}_1$ and $\tilde{x}_2$ are then sent to the ML decoder to estimate the transmitted symbols x_1 and x_2, respectively.

2.6. Wireless Communication Channel

Communication signals are transmitted through different sorts of channels. For the purpose of designing and optimizing receiver structures for digital communication systems it is required to build mathematical models that represent the typical characteristics of these channels. In this thesis, AWGN channel and Rayleigh fading channel models will be utilized.

2.6.1. Additive White Gaussian Noise Channel

Additive white Gaussian noise channel is the least complex model of the communication channel. This kind of noise is created by the electronic components at the receiver, e.g., the amplifier. If the noise is introduced by electronic components and amplifiers at the receiver, it it tends to be characterized as thermal noise. This sort of noise is characterized statistically by a Gaussian process [37].

AWGN channel model comprises of a transmitted signal $s(t)$ and an additive noise process $n(t)$ as appeared in Figure 2.10.

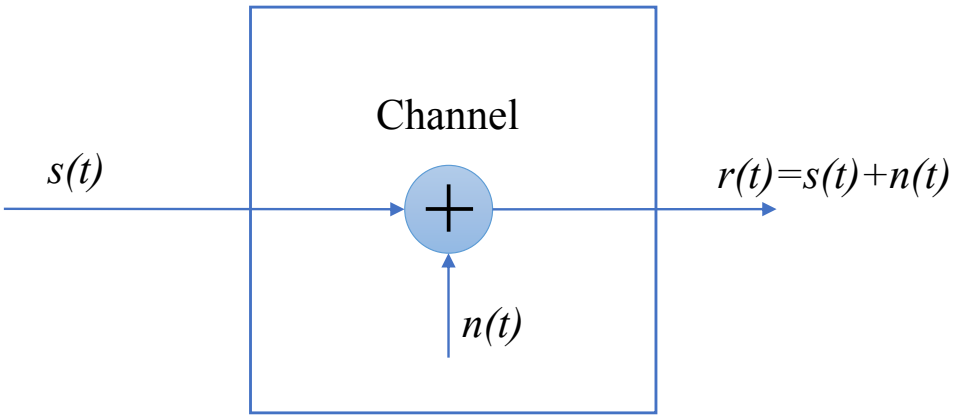

Figure 2.10. AWGN channel model.

2.6.2. Rayleigh Fading Channel

Over the most recent three decades, there has been a wide range of ways to deal with the modeling and simulation of mobile radio channels, see [38], [39] and the references therein. Among them, the well-known mathematical reference model due to Clarke [38] and its simplified simulation model due to Jakes [40] have been broadly used for Rayleigh fading channels for around 30 years.

The Rayleigh distribution is frequently used to model multipath fading with no direct line-of-sight path between transmitter and receiver antennas. The received envelope of a flat fading signal or the envelope of an individual multipath component is given by Rayleigh distribution with probability density function (PDF) of channel fading amplitude α as

$$f_{\alpha}(\alpha) = \frac{\alpha}{\sigma^2} e^{\left(\frac{-\alpha^2}{2\sigma^2}\right)}, \alpha \geq 0, \tag{2.31}$$

where σ is the standard deviation and σ^2 is the variance of the received signal before detection. Rayleigh fading exists in urban communication area where there is no line-of-sight communication.

3. RELIABILITY AND SI-ASSISTED DECODING STRATEGY

In this chapter, we provide the system model with all details about the strategies and methods adopted for both transmitter and receiver processing. Herein, detailed derivations and analytical expressions related with the proposed scheme are visited.

3.1. System Model

We consider a downlink MU-MIMO wireless system model as shown in Figure 3.1, where a transmitter (Base Station, BS) equipped with N transmit antennas attempts to communicate K equal size packets $\{p_1, p_2, \ldots, p_K\}$ to single-antenna receivers (User Equipment, UE). The set of UEs is denoted as $k = \{1, 2, \ldots, K\}$.

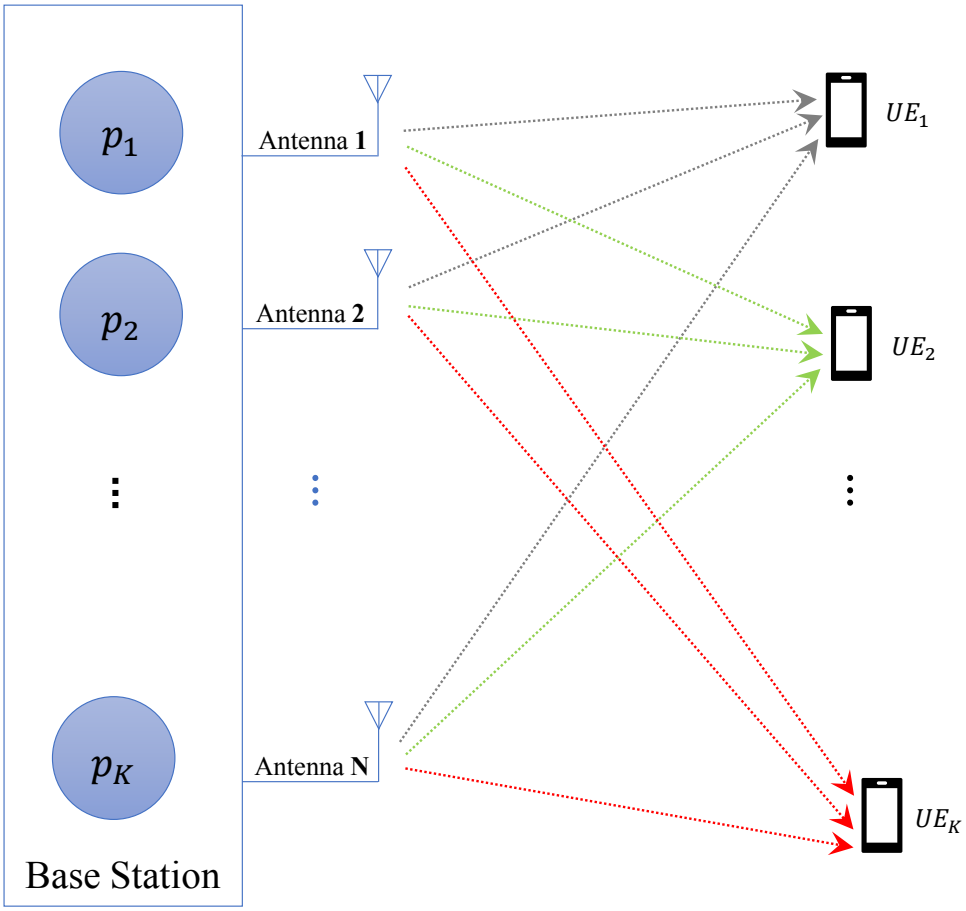

Figure 3.1. Basic system model.

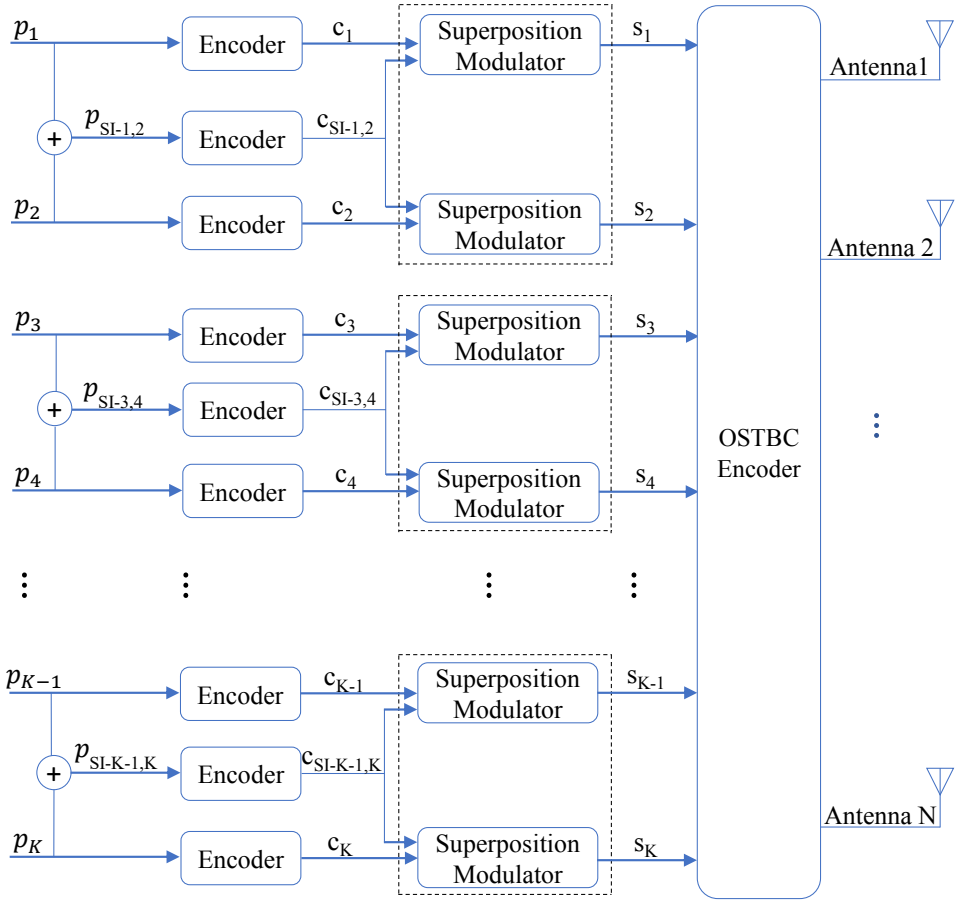

Figure 3.2. Transmitter architecture.

3.2. Highly-Reliable XOR-assisted Transmission with New Encoded OSTBC Approach

3.2.1. Transmitter Processing

Following similar side information (SI)-assisted error recovery techniques considered in [41], the same network coding (NC) methodology used for a pair of users (UE_1, UE_2) is adapted for each two successive users in our proposed downlink MU-MIMO wireless system model. Similarly, the SI is disseminated through the use of superposition modulation to avoid the use of any extra physical resources and thus, the overall spectral efficiency is not decreased.

Figure 3.2 shows the basic transmitter processing for transmitting a number of K equal size packets $\{p_1, p_2, \ldots, p_K\}$ to a set of K UEs. K, which represents the number of UEs supported by the system and equivalently the number of packets, is defined according to the new encoded OSTBC approach code which is basically related to the number of transmitting antennas (N) at the BS. The number of UEs is strictly considered to be an even number. The restriction ensures the deployment of the side information packets $p_{SI-i,i+1}$, which are the bit-level XOR-ed of the main two successive user packets p_i and p_{i+1}, where i is odd and $i \in \{1, 3, \ldots, K-1\}$.

First, packets p_i, p_{i+1} and $p_{SI-i,i+1} = p_i \oplus p_{i+1}$ are encoded independently by rate-R convolutional encoder to produce the coded bit sequences c_i, c_{i+1} and $c_{SI-i,i+1}$, where i is odd and $i \in \{1, 3, \ldots, K-1\}$. Then, the generated code streams are fed into the symbol mapper to produce the transmit symbols for the K set of users. Superposition modulation is employed in such a way that each three coded bit sequences c_i, c_{i+1} and $c_{SI-i,i+1}$ are mapped to two composite constellation symbol sequences s_i and s_{i+1}, where i is odd and $i \in \{1, 3, \ldots, K-1\}$ using only one physical resource $\mathcal{R}$ since a new OSTBC encoder approach is considered in the next processing stage.

3.2.2. Superposition Modulation and Constellation Design

Following a similar procedure as laid out in [41], [42], a superposition constellation can be obtained by suitably combining two uniform-QAM constellations.

$$s_i = \sqrt{1-\alpha}x_1 + \sqrt{\alpha}x_2,\ i \in \{1, 2, \ldots, K\}, \tag{3.1}$$

where x_1 and x_2 are the constituent complex symbols, for example, m-QAM and the parameter $0 \leq \alpha \leq 1$ is the power split between the two constellations. With the deter-

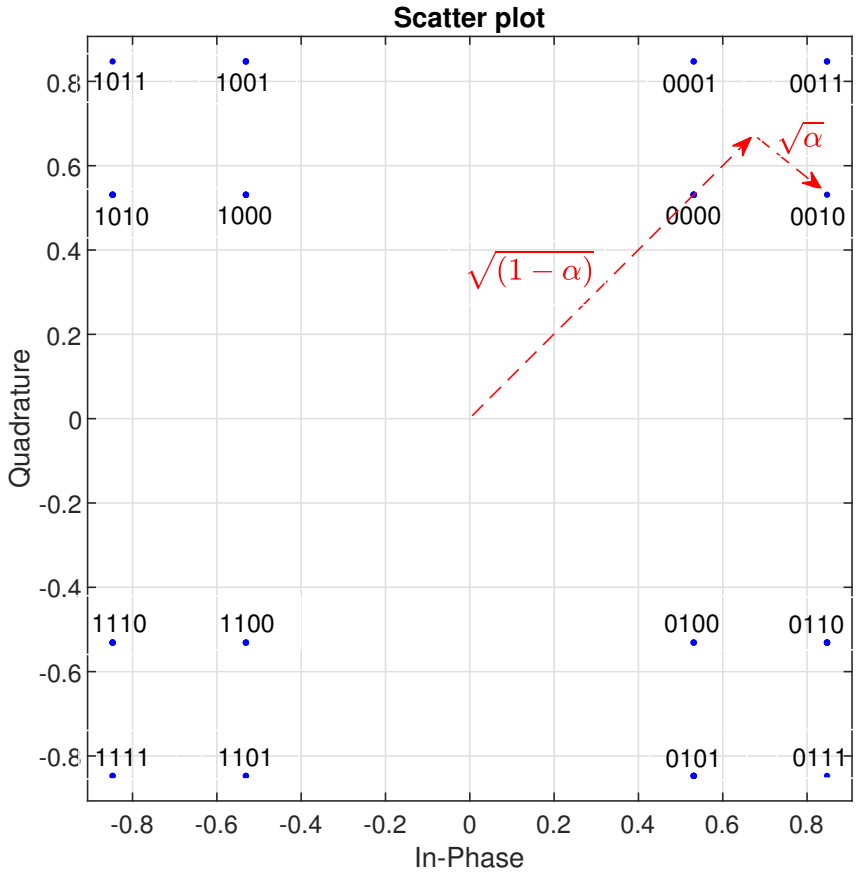

Figure 3.3. Composite constellation with Gray mapping $\alpha = 0.05$.

mination of α and the component (primary) modulations, the composite constellation is formed. Figure 3.3 demonstrates a non-uniform composite constellation generated because of superimposition of two 4-QAM constellations with power split $\alpha = 0.05$. The superposition modulation is implemented such that, the number of $m_c^{(MSB)}$ bits from c_i or c_{i+1} is gathered with a number of $m_c^{(LSB)}$ bits from $c_{SI-i,i+1}$, i is odd and $i \in \{1, 3, \ldots, K-1\}$ to build a complex symbol. The resulting composite constellation has a size of $M = 2^{(m_c^{(MSB)}+m_c^{(LSB)})}$ where the most significant bits (MSBs) and the least significant bits (LSBs) of each symbol are represented by the $m_c^{(MSB)}$ and $m_c^{(LSB)}$, respectively. For our proposed system model two lower order 4-QAM constellations are adopted such that $m_c^{(MSB)} = m_c^{(LSB)} = 2$, resulting in a 16 points composite constellations. For this situation, the quadrant of the transmitted symbol is specified by the bits from c_i or c_{i+1}, while the bits from $c_{SI-i,i+1}$ decide the correct area of the transmitted symbol in the quadrant.

3.2.3. MU-MIMO New Encoded OSTBC Approach

A systematic design method to generate high rate complex orthogonal space-time block codes (STBCs) for any number of transmit antennas as presented in [43] is used for our system model, however, with a new approach.

The proposed STBC is described with a $P \times N$ transmission matrix G_N, the entries of the matrix G_N are linear combinations of the precise users' symbols $\{s_1, s_2, \ldots, s_K\}$ and their conjugates, where P refers to the block length of the matrix, N and K represent the number of transmit antennas and number of users, respectively. In this work, we consider G_2 and G_4 which represent codes that utilize two and four transmitting antennas, respectively. According to the systematic design algorithm to generate high rate complex orthogonal STBCs for any number of transmit antennas, G_2 and G_4 are given by

$$G_2 = \begin{bmatrix} s_1 & s_2 \\ -s_2^* & s_1^* \end{bmatrix}, \tag{3.2}$$

$$G_4 = \begin{bmatrix} s_1 & s_2 & s_3 & 0 \\ -s_2^* & s_1^* & 0 & s_4^* \\ -s_3^* & 0 & s_1^* & s_5^* \\ 0 & -s_3^* & s_2^* & s_6^* \\ 0 & -s_4 & -s_5 & s_1 \\ s_4 & 0 & -s_6 & s_2 \\ s_5 & s_6 & 0 & s_3 \\ -s_6^* & s_5^* & -s_4^* & 0 \end{bmatrix}. \tag{3.3}$$

As stated earlier, our transmission model uses a superposition modulation with a total of $M = 2^b$ composite constellation elements. In one time slot, b specific user bits reach the encoder and the appropriate constellation signal corresponding to that user is picked, by setting s_i as the constellation symbol selected for a specific bits of user k, $i = k$ and $i \in \{1, 2, \ldots, K\}$, a matrix G_N is realized with entries as linear combinations of $\{s_1, s_2, \ldots, s_K\}$ and their conjugates. Here, K is the number of users that can be supported by the MU-MIMO system for a chosen number of transmit antennas N,

which can be defined also by how many different entries s_i are generated in the matrix G_N. For G_2 and G_4, the proposed system accommodates $K = 2$ and $K = 6$ users, respectively.

As P time slots are used to transmit one symbol for each user, the rate of the code is $1/P$, resulting in $1/2$ and $1/8$ code rates for G_2 and G_4, respectively. One can notice that the rates are low when compared to the use of conventional OSTBC, where the rates can be defined as 1 and $3/4$ for G_2 and G_4, respectively. Basically, the orthogonality of the columns of G_N for this specific MU-MIMO OSTBC approach allows the application of a simple linear decoding scheme at the receiver and also the use of only one common physical resource $\mathcal{R}$ for all users.

3.2.4. Decoding Algorithm and Sub-Constellation Alignment for Signal Combining

A sub-constellation alignment approach is presented and investigated in [41] for useful joining of LSBs of the received symbols to guarantee proper delivery of SI. The sub-constellation alignment for signal combining procedure is modified for the new MU-MIMO encoded OSTBC system model considered in this work. Figure 3.4 demonstrates the general construction of the receiver.

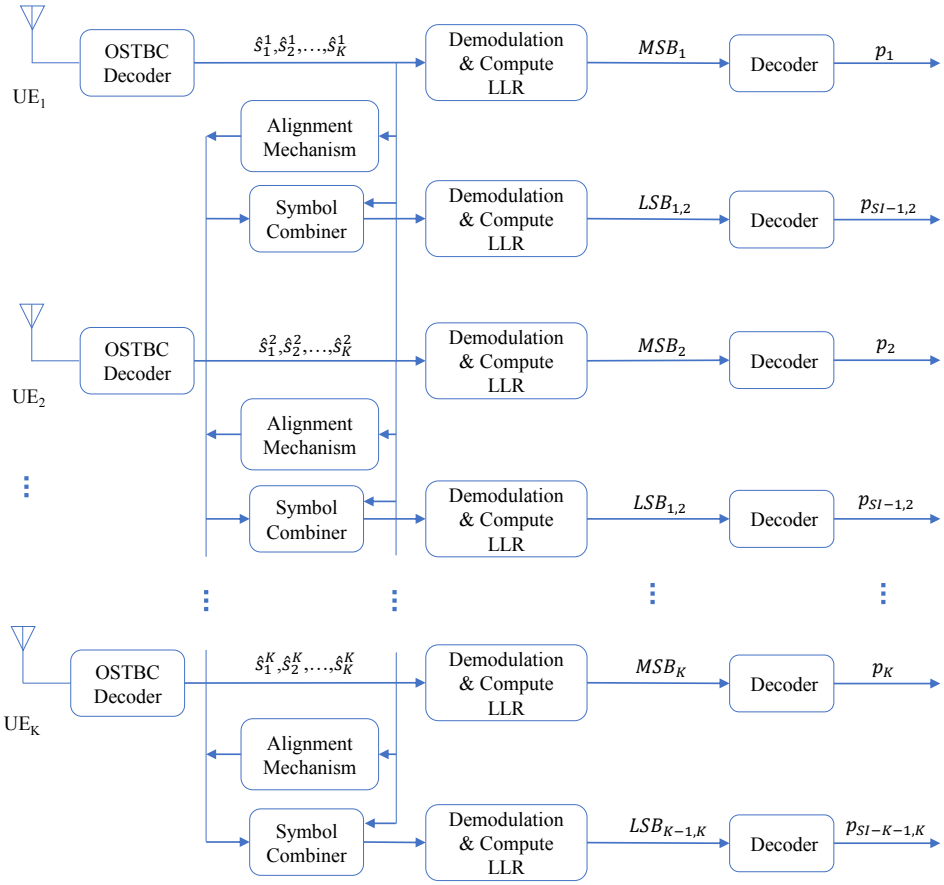

Figure 3.4. Receiver architecture.

As shown earlier, for $N = 2$ transmitting antennas, a G_2 matrix is generated as in (3.2). In this case, $K = 2$ single-antenna UEs are served, and the received signals are given by

$$\begin{cases} y_k^1 = h_{1,k}s_1 + h_{2,k}s_2 + n_k^1, & \text{at time one,} \\ y_k^2 = -h_{1,k}s_2^* + h_{2,k}s_1^* + n_k^2, & \text{at time two, } k \in \{1,2\}. \end{cases} \tag{3.4}$$

The coefficient $h_{1,k}$ is the channel from transmit antenna one to receive antenna of user k and $h_{2,k}$ is the channel from transmit antenna two to receive antenna of user k. Noise terms n_k^1 and n_k^2 are AWGN of receiver k with zero mean and variance N_0 at time one and two, respectively. The OSTBC combining scheme builds the following two signals at the level of each user k

$$\begin{cases} \hat{s}_1^k = y_k^1 h_{1,k}^* + y_k^{2*} h_{2,k}, \\ \hat{s}_2^k = y_k^1 h_{2,k}^* - y_k^{2*} h_{1,k}, \quad k \in \{1,2\}. \end{cases} \tag{3.5}$$

Similarly, the combining scheme for the MU-MIMO new encoded OSTBC approach can be generalized for any number of transmitting antennas N, in this case, K users are considered. Thus, according to the STBC combining scheme signals $\{\hat{s}_1^k, \hat{s}_2^k, \ldots, \hat{s}_K^k\}$ are built at the level of each receiver k, $k \in \{1, 2, \ldots, K\}$.

As expressed before, the data relating to packets $\{p_1, p_2, \ldots, p_K\}$ are transmitted utilizing MSBs of the transmitted composite constellation symbols. In this manner, it is less likely to make a mistake in decoding the main packets $\{p_1, p_2, \ldots, p_K\}$ than $p_{SI-i,i+1}$, i is odd and $i \in \{1, 3, \ldots, K-1\}$ which depends on a transmission with smaller Euclidean distance. Nevertheless, since the equivalent c_{SI} is transmitted within the composite symbols of every two successive users $(k, k+1)$, k is odd and $k \in \{1, 3, \ldots, K-1\}$, these can be joined to compensate the loss for being sent with smaller Euclidean distance.

After building $\{\hat{s}_1^k, \hat{s}_2^k, \ldots, \hat{s}_K^k\}$ signals at the level of each user k, our main issue is the combining technique. However, since the MSBs of the successive transmitted composite symbols s_i and s_{i+1}, i is odd and $i \in \{1, 3, \ldots, K-1\}$ are not the same, an immediate combining is not conceivable. To address this issue an arrangement or phase alignment should be performed before the combining procedure. The alignment mechanism should be performed on the OSTBC combined symbols $\{\hat{s}_1^k, \hat{s}_2^k, \ldots, \hat{s}_K^k\}$ built at the level of every receiver k as

$$\bar{s}_i^k = \begin{cases} Sgn(Re(\hat{s}_i^k)) \prod_{j=1, j\neq k}^{K} Sgn(Re(\hat{s}_{i+1}^j)) Re(\hat{s}_i^k) + \Im \\ Sgn(Im(\hat{s}_i^k)) \prod_{j=1, j\neq k}^{K} Sgn(Im(\hat{s}_{i+1}^j)) Im(\hat{s}_i^k), \\ \text{for } i \text{ odd}, \\ Sgn(Re(\hat{s}_i^k)) \prod_{j=1, j\neq k}^{K} Sgn(Re(\hat{s}_{i-1}^j)) Re(\hat{s}_i^k) + \Im \\ Sgn(Im(\hat{s}_i^k)) \prod_{j=1, j\neq k}^{K} Sgn(Im(\hat{s}_{i-1}^j)) Im(\hat{s}_i^k), \\ \text{for } i \text{ even}, \end{cases} \tag{3.6}$$

where $i \in \{1, 2, \ldots, K\}$ and $k \in \{1, 2, \ldots, K\}$. $\Im = \sqrt{-1}$, $Sgn(x)$, $Re(x)$ and $Im(x)$ represent sign, real and imaginary functions, respectively.

After the sub-constellation alignment, the combined signals $s^k_{i,Comb}$ can be computed as

$$s^k_{i,Comb} = \begin{cases} \hat{s}^k_i + \sum\limits_{m=1,m\neq k}^{K} \bar{s}^m_{i+1}, \text{for } i \text{ odd}, \\ \hat{s}^k_i + \sum\limits_{m=1,m\neq k}^{K} \bar{s}^m_{i-1}, \text{for } i \text{ even}, \end{cases} \tag{3.7}$$

where $i \in \{1, 2, \ldots, K\}$ and $k \in \{1, 2, \ldots, K\}$.

We provide the decoding formula for each symbol for the general case of N transmit antennas and K users. The maximum likelihood detection amounts to minimizing the decision statistic

$$|s^k_{i,Comb} - s_j|^2 + (-1 + \sum_{m=1}^{K}\sum_{n=1}^{N} |h_{n,m}|^2)|s_j|^2 \tag{3.8}$$

over all possible values of constellation symbols s_j for decoding $s^k_{i,Comb}$, where $h_{n,m}$ is the channel from transmit antenna n to receive antenna of user m, $i \in \{1, 2, \ldots, K\}$ and $k \in \{1, 2, \ldots, K\}$.

3.2.5. SI-assisted Decoding Strategy

As a consequence of the new MU-MIMO encoded OSTBC approach, UE_k not only receives its own symbol but all other users' transmitted symbols, the offered diversity allows the recovery of a specific user packet in different ways. If K users are considered, for each UE_k, $k \in \{1, 2, \ldots, K\}$, we provide $2K$ different ways to recover the user specific packet p_i. As an example, for $N = 2$ transmitting antennas, implies $K = 2$ users in the downlink. First, UE_1 endeavors to decode c_1, in case of a decoding error, UE_1 sets out on decoding c_2 and $c_{SI-1,2}$, on the off chance that decoding of both c_2 and $c_{SI-1,2}$ are effective, UE_1 obtains p_1 from successfully decoded p_2 and $p_{SI-1,2}$. However, if there is an error in decoding both c_2 and $c_{SI-1,2}$, UE_1 has two additional chances to decode p_1 since UE_2 is receiving a second version of the transmitted packets. Now, the focus is to decode c_1 received by the second user. In the event of a decoding error the last option for the first user is to decode c_2 and $c_{SI-1,2}$, with the condition that decoding of both are fruitful, UE_1 recovers p_1, but if either of the two are decoded erroneously, UE_1 considers the packet p_1 as lost.

Let us consider the same example, where the BS is equipped with two transmitting antennas and two users are considered. Let $P^{(i)}_{e,k}$, $k \in \{1, 2\}$ and $i \in \{1, 2, SI-1, 2\}$, indicate the probability of error in decoding packet p_i of user k. $P^{(i)}_{c,NC}$ signifies the probability of correct recovery of p_i and can be just expressed as

$$\begin{aligned} P^{(i)}_{c,NC} = 1 - P^{(i)}_{e,1} + P^{(i)}_{e,1}\big(1 - P^{(j)}_{e,1}\big)\big(1 - P^{(SI-1,2)}_{e,1}\big) + P^{(i)}_{e,1}\big(1 - P^{(j)}_{e,1}\big)\big(1 - P^{(SI-1,2)}_{e,1}\big)P^{(i)}_{e,2} \\ + P^{(i)}_{e,1}\big(1 - P^{(j)}_{e,1}\big)\big(1 - P^{(SI-1,2)}_{e,1}\big)P^{(i)}_{e,2}\big(1 - P^{(j)}_{e,2}\big)\big(1 - P^{(SI-1,2)}_{e,2}\big), \end{aligned} \tag{3.9}$$

for $i, j \in \{1, 2\}, i \neq j$. In (3.9), we estimate $P_{e,k}^{(i)}$ and $P_{e,k}^{(j)}$ to be mutually exclusive from $P_{e,k}^{(SI-1,2)}$. Consequently, the probability of error of p_i is denoted as $P_{e,NC}^{(i)}$, which is $P_{e,NC}^{(i)} = 1 - P_{c,NC}^{(i)}$, is given by

$$P_{e,NC}^{(i)} = P_{e,1}^{(i)}\big[P_{e,1}^{(j)} + P_{e,1}^{(SI-1,2)} - P_{e,1}^{(j)}P_{e,1}^{(SI-1,2)}\big] \\ - P_{e,1}^{(i)}\big(1 - P_{e,1}^{(j)}\big)\big(1 - P_{e,1}^{(SI-1,2)}\big)P_{e,2}^{(i)}\big[1 + \big(1 - P_{e,2}^{(j)}\big)\big(1 - P_{e,2}^{(SI-1,2)}\big)\big]. \quad (3.10)$$

Equation (3.10) can be rewritten in the same manner with the possibility to consider the general model with N transmit antennas and K users.

4. SIMULATION RESULTS AND DISCUSSION

In this chapter, simulation results for specific scenarios based on the system model, well described in the previous chapter, are presented and followed by discussions.

4.1. Simulation Parameters

A rate-1/3 convolutional encoder, $[133, 171, 165]_8$ with constraint length 6 is employed along with superposition modulation with the choice of $m_c^{(MSB)} = m_c^{(LSB)} = 2$, which results in a 16 point Gray mapping composite constellation that is composed of two lower order 4-QAM constellations, the power parameter α is chosen to be 0.05 and 0.10. The block length is set to 100 bits and the channels involved are modeled by independent Rayleigh fading $\mathcal{CN}(0, 1)$. The soft-decision Viterbi decoding is carried out at the receiver side.

4.2. Simulation Results

In the following, we provide simulation results in order to validate the error performance improvement for two different MU-MIMO transmission scenarios.

In all the BLER figures provided in this section, the legend entries $P_{i,NC}$ and P_i refer to the error performance of packet p_i of any user k, where $i \in \{1, 2, \ldots, K\}$ and similarly $k \in \{1, 2, \ldots, K\}$, with and without the SI-assisted decoding strategy (detailed for the case of first scenario in subsection 3.2.5), respectively. For the evaluation of "LSB signal combined" the performance of P_{SI} for any arbitrary $p_{SI-i,i+1}$, i is odd and $i \in \{1, 3, \ldots, K-1\}$, is considered as well, while the legend section "Lower-Bound" illustrates the anticipated lower bound (as given by (3.10) for the case of the first scenario) as a reference for comparison.

4.2.1. Results with New Encoded OSTBC Approach

4.2.1.1. First Scenario

In the first scenario we consider two transmitting antennas at the base station, G_2 is considered for the new encoded OSTBC approach with rate $1/2$ and two users can be accommodated by the system. We assume that the same amount of energy is shared by the transmitting antennas to guarantee that the same aggregate power is utilized in both scenarios, where $\frac{E_s}{N_0} = \frac{1}{2}$ is the average power of the composite constellation for the first scenario.

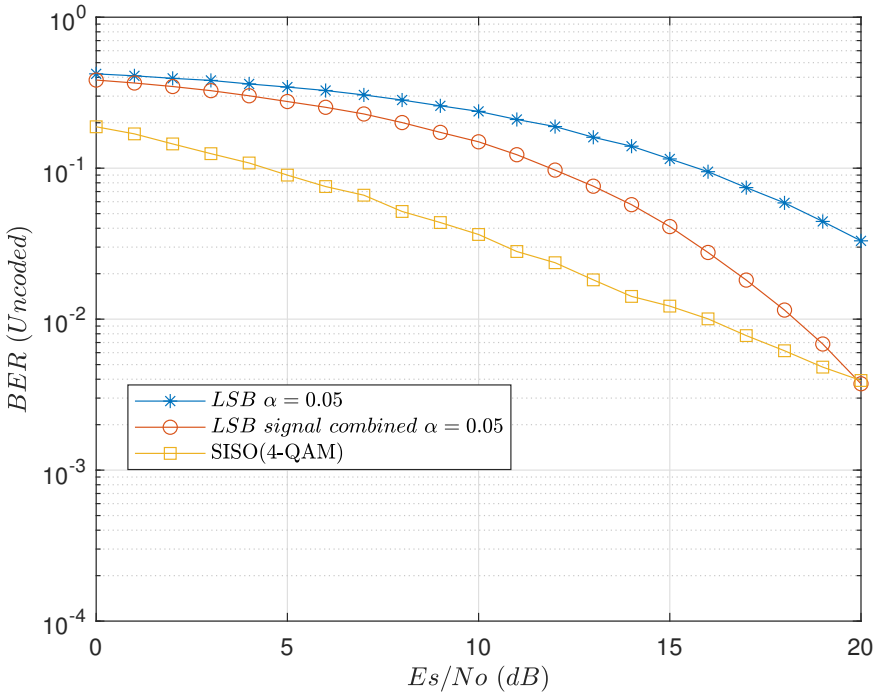

Figure 4.1. Un-coded BER performance for the case of two transmitting antennas with new encoded OSTBC approach and $\alpha = 0.05$.

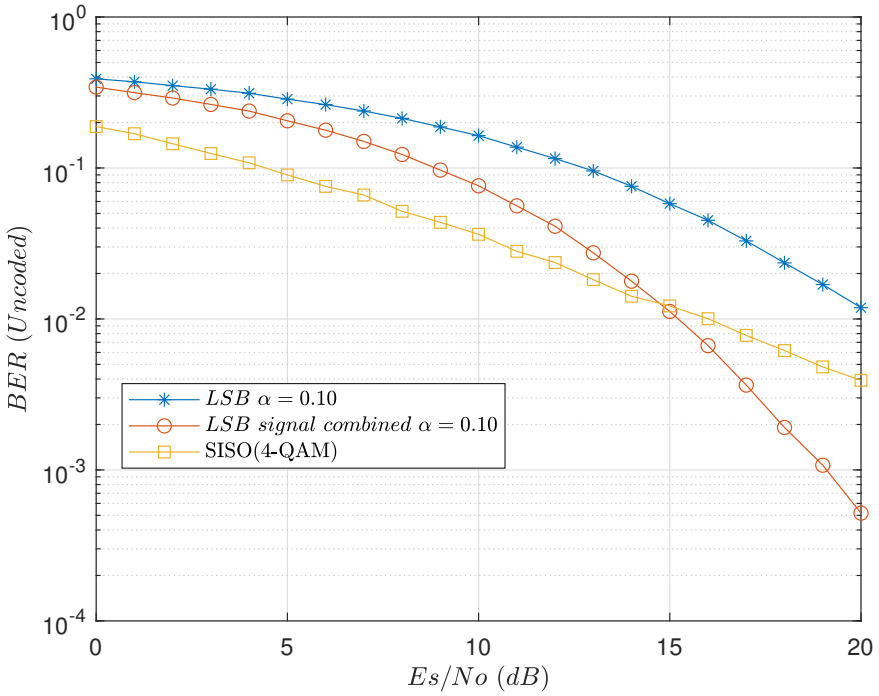

Figure 4.2. Un-coded BER performance for the case of two transmitting antennas with new encoded OSTBC approach and $\alpha = 0.10$.

Figure 4.1 and Figure 4.2 show the un-coded bit error rate (BER) performance over $\frac{E_s}{N_0}$ related to the first scenario ($N = 2$ and $K = 2$) for two different values of $\alpha = 0.05$ and $\alpha = 0.10$, respectively. The figures confirm that the proposed combining of the received signals results in a significant gain that even exceeds the performance of the baseline 4-QAM at higher $\frac{E_s}{N_0}$. In case $\alpha = 0.10$, the gain is more significant and considerably at less $\frac{E_s}{N_0}$ compared to the case where $\alpha = 0.05$.

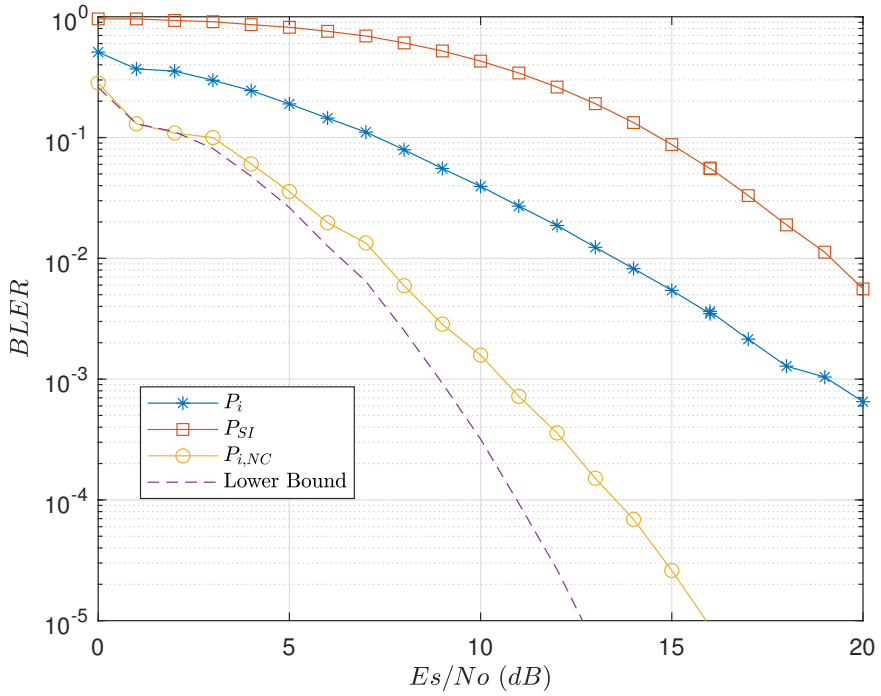

Figure 4.3. BLER performance for the case of two transmitting antennas with new encoded OSTBC approach and $\alpha = 0.05$.

Figure 4.3 and Figure 4.4 demonstrate the block error rate (BLER) performance over $\frac{E_s}{N_0}$ corresponding to the first scenario ($N = 2$ and $K = 2$) for two different estimations of $\alpha = 0.05$ and $\alpha = 0.10$, respectively. To verify the performance gains promised by the proposed new encoded OSTBC approach for a MU-MIMO scenario and appropriate combining of received signals for error recovery, one can refer to [41]; hence a significant achieved performance gain can be clearly seen. This is due to the additional diversity offered by the new encoded OSTBC approach, where each user is receiving all other users symbols. On one hand, this fact will enhance the alignment mechanism for signal combining which now exploits the all other users channels and, on the other hand, several chances for the recovery of packet p_i of user k are offered, $2K$ $(= 4)$ alternative ways; hence reliability is strongly supported.

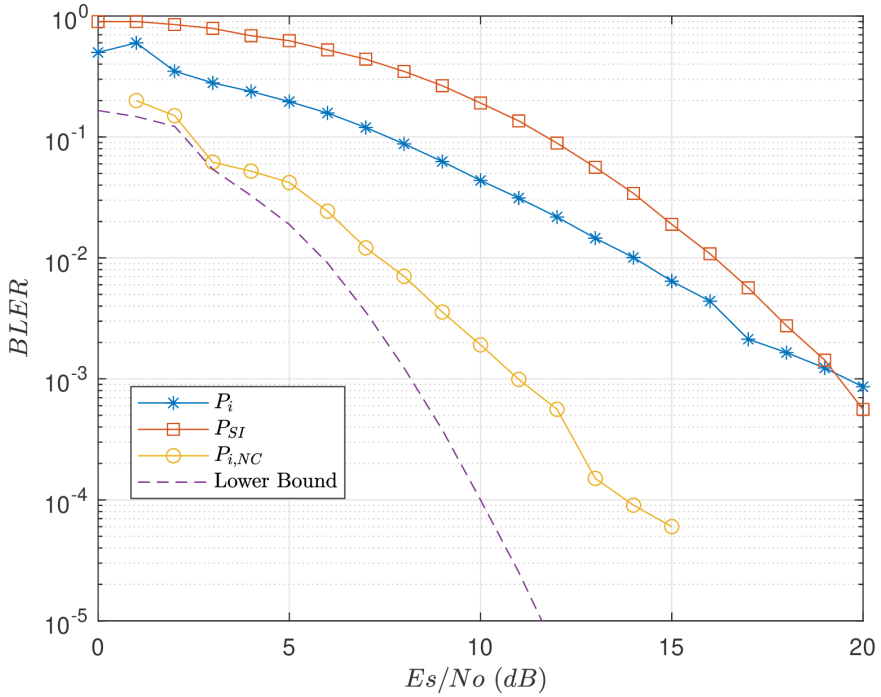

Figure 4.4. BLER performance for the case of two transmitting antennas with new encoded OSTBC approach and $\alpha = 0.10$.

Figure 4.4 shows the impact of picking α, the figure affirms the noteworthy P_{SI} gain by the proposed signal combining, that even outperforms the performance of P_i at higher E_s/N_0 for $\alpha = 0.10$. However, α should be picked in such away to help a moderately comparable performance for p_i and $p_{SI-i,i+1}$ transmission. A poorly chosen value of α would sway the power to one of the constitute constellations that leads to a degradation of the overall performance.

4.2.1.2. Second Scenario

In the second scenario, four transmitting antennas are utilized at the base station, which involves the use of G_4 for the new encoded OSTBC approach with rate $1/8$, and six users are considered. We assume that the same amount of energy is shared by the transmitting antennas to guarantee that the same aggregate power is utilized in both scenarios, where $\frac{E_s}{N_0} = \frac{1}{4}$ is the average power of the composite constellation for the second scenario.

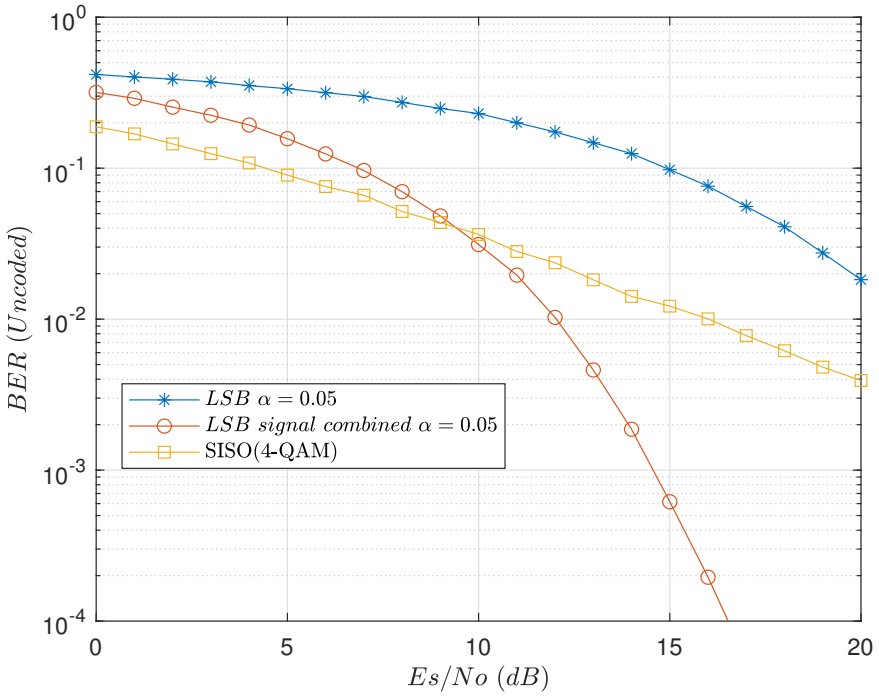

Figure 4.5. Un-coded BER performance for the case of four transmitting antennas with new encoded OSTBC approach and $\alpha = 0.05$.

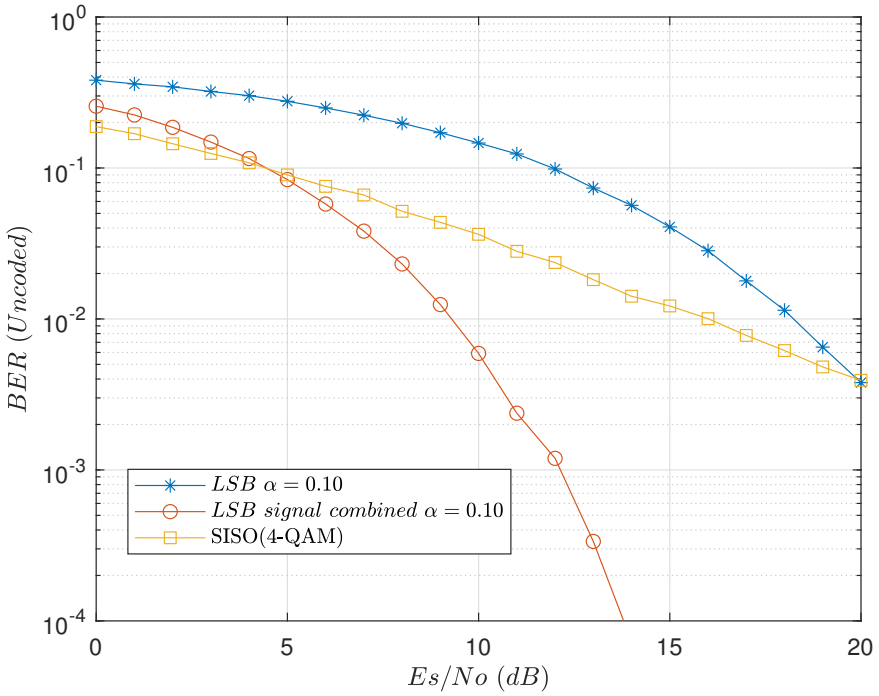

Figure 4.6. Un-coded BER performance for the case of four transmitting antennas with new encoded OSTBC approach and $\alpha = 0.10$.

Figure 4.5 and Figure 4.6 present the un-coded bit error rate (BER) performance over $\frac{E_s}{N_0}$ corresponding to the second scenario ($N = 4$ and $K = 6$) for two estimations of $\alpha = 0.05$ and $\alpha = 0.10$, respectively. We notice that the performance of the combining of the received signal is significantly enhanced when compared to the first scenario. This is caused by the fact that now more users are supported by the system, which strengthens the LSB signal combining as the alignment mechanism relies on the channel estimates of all users.

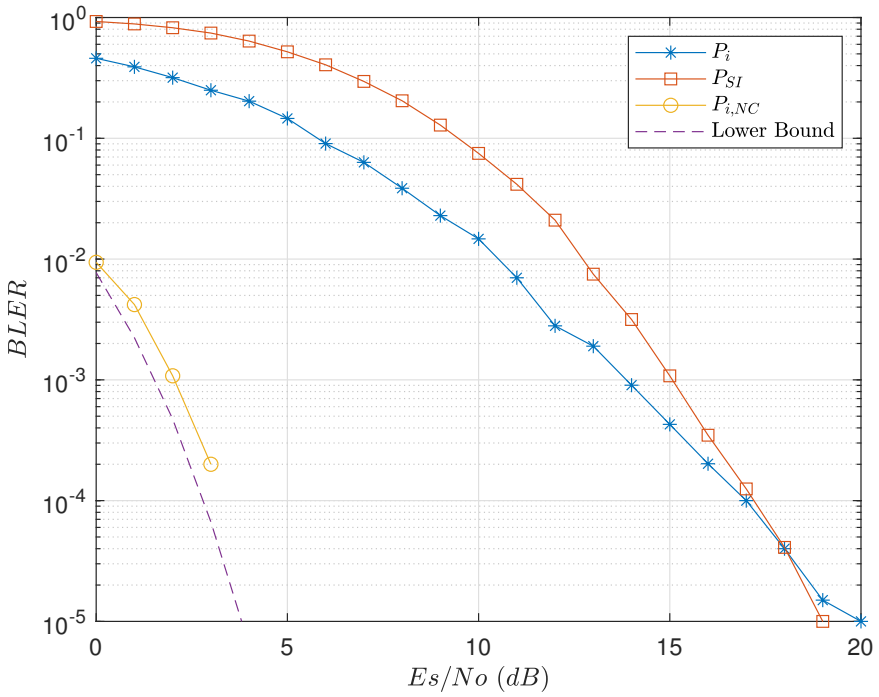

Figure 4.7. BLER performance for the case of four transmitting antennas with new encoded OSTBC approach and $\alpha = 0.05$.

Figure 4.7 and Figure 4.8 show the block error rate (BLER) performance over $\frac{E_s}{N_0}$ corresponding to the second scenario ($N = 4$ and $K = 6$) for two different values of $\alpha = 0.05$ and $\alpha = 0.10$, respectively. We observe that the performance is significantly improved when compared to the first scenario. Despite the fact that the rate of the new encoded OSTBC code is brought down to $1/8$, more users are supported by the system which strengthens the LSB signal combining and provides $2K(= 12)$ alternative attempts for user packet recovery.

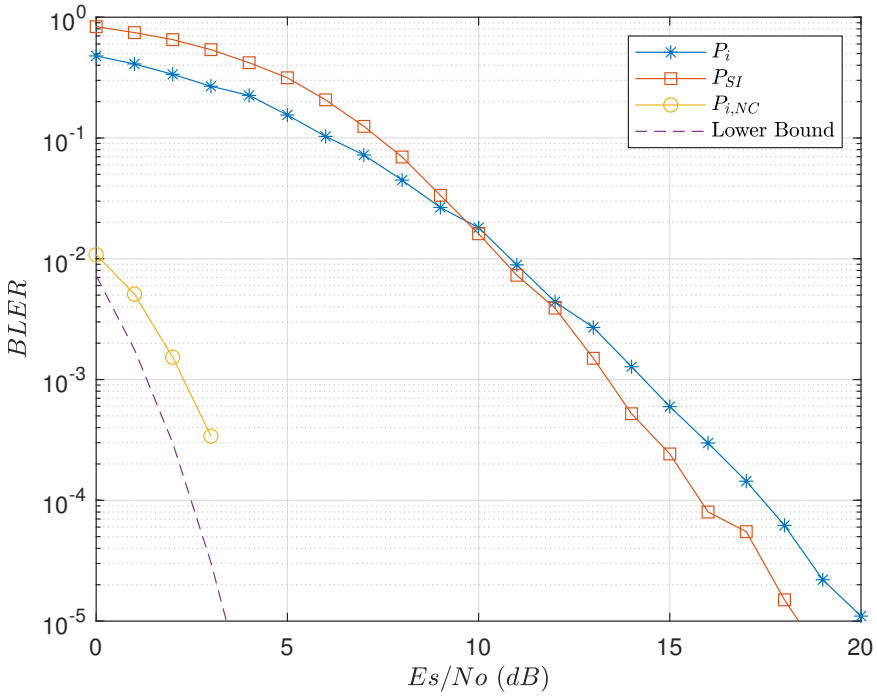

Figure 4.8. BLER performance for the case of four transmitting antennas with new encoded OSTBC approach and $\alpha = 0.10$.

4.2.2. Results with Conventional OSTBC

As a global evaluation for the proposed system, multiple users can be accommodated by sharing just a single resource; furthermore, as more users are added, a higher reliability is promised. Apart from that, one can consider the fact of lowering the transmission rate where latency comes into account. To compensate for the low rates, simulation is conducted for both scenarios where conventional OSTBC is used with rates 1 and $3/4$ for G2 and G4, respectively. As a penalty to pay, K orthogonal resources are needed for K users.

4.2.2.1. First Scenario

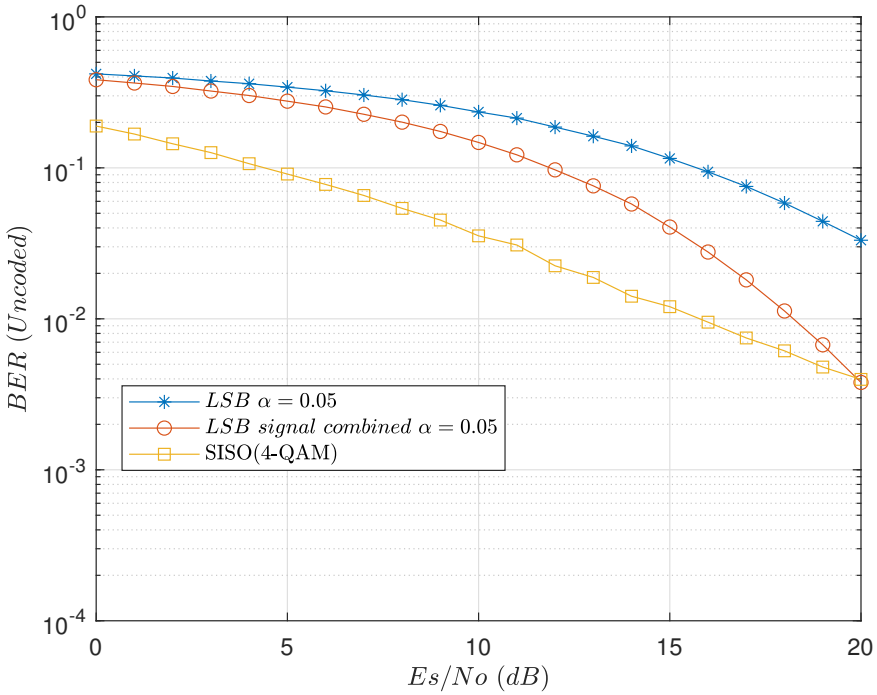

Figure 4.9. Un-coded BER performance for the case of two transmitting antennas with conventional encoded OSTBC and $\alpha = 0.05$.

Figure 4.9 and Figure 4.10 illustrate the un-coded bit error rate (BER) performance versus $\frac{E_s}{N_0}$ where $N = 2$ and $K = 2$ and conventional encoded OSTBC is used for two estimations of $\alpha = 0.05$ and $\alpha = 0.10$, respectively. It can be observed that the same gain performance is achieved by the combining scheme when compared to the first scenario where the new encoded OSTBC approach is used (Figure 4.1 and Figure 4.2).

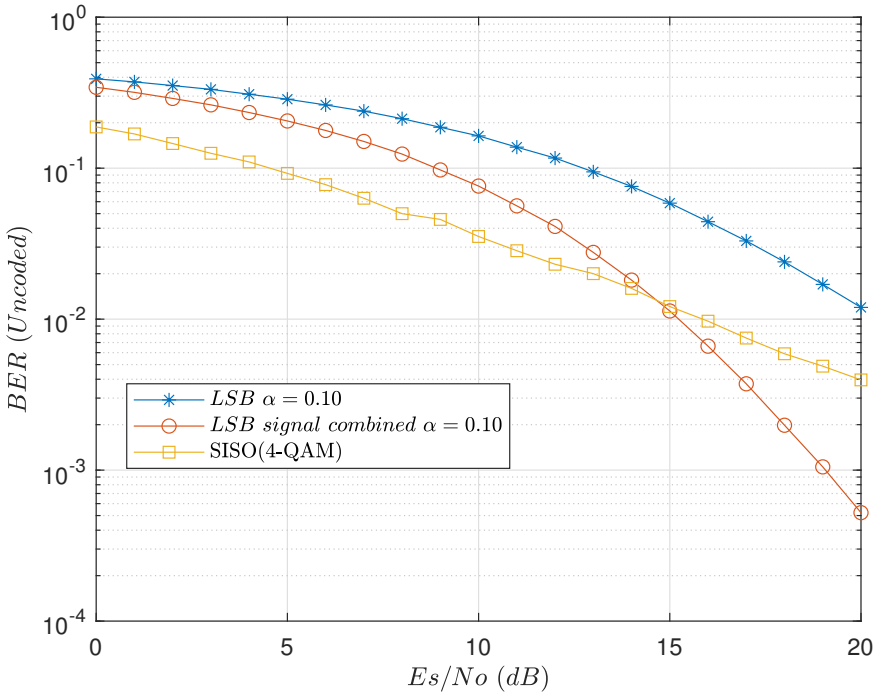

Figure 4.10. Un-coded BER performance for the case of two transmitting antennas with conventional encoded OSTBC and $\alpha = 0.10$.

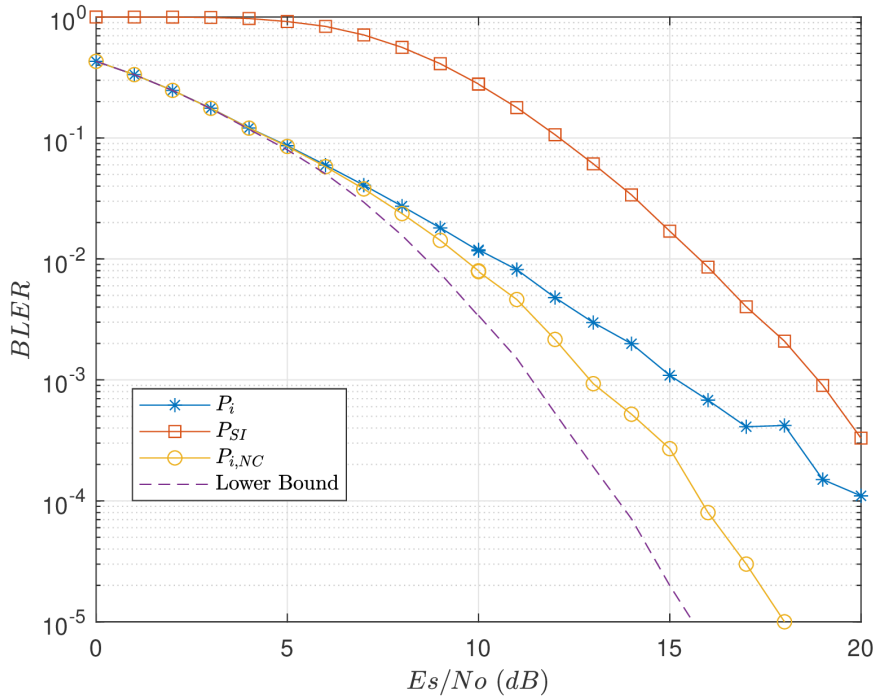

Figure 4.11. BLER performance for the case of two transmitting antennas with conventional encoded OSTBC and $\alpha = 0.05$.

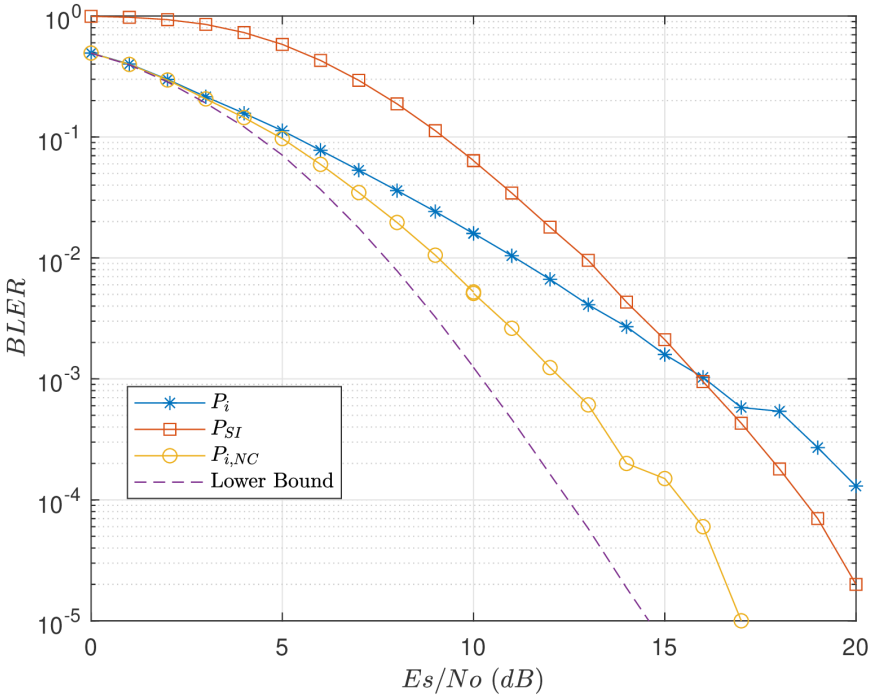

Figure 4.12. BLER performance for the case of two transmitting antennas with conventional encoded OSTBC and $\alpha = 0.10$.

Figure 4.11 and Figure 4.12 present the block error rate (BLER) performance over $\frac{E_s}{N_0}$ for the situation where $N = 2$, $K = 2$ and conventional OSTBC is used for two different values of $\alpha = 0.05$ and $\alpha = 0.10$, respectively. Comparing Figure 4.11 and Figure 4.12 with Figure 4.3 and Figure 4.4, we notice the performance gain accomplished by P_i and P_{SI} when conventional OSTBC is used. In Figure 4.11 and Figure 4.12, the performance effect of $P_{i,NC}$ is apparent at a considerable higher E_s/N_0 range. However, the performance achieved is less comparable with results shown in Figure 4.3 and Figure 4.4 where the new encoded OSTBC approach is considered. This can be justified by the fact that the diversity offered by the new encoded OSTBC (a user not only receives its own symbol but all other users transmitted symbols) no longer exists, by utilizing the classical OSTBC every user is just receiving its own symbol. Thus, the alignment mechanism and symbol combining is valid only between two successive users, or in other words, the alternative endeavors given by the SI-assisted decoding strategy do not rely upon the number of users K, only two different ways for packet recovery are possible regardless of the number of users in the system.

4.2.2.2. Second Scenario

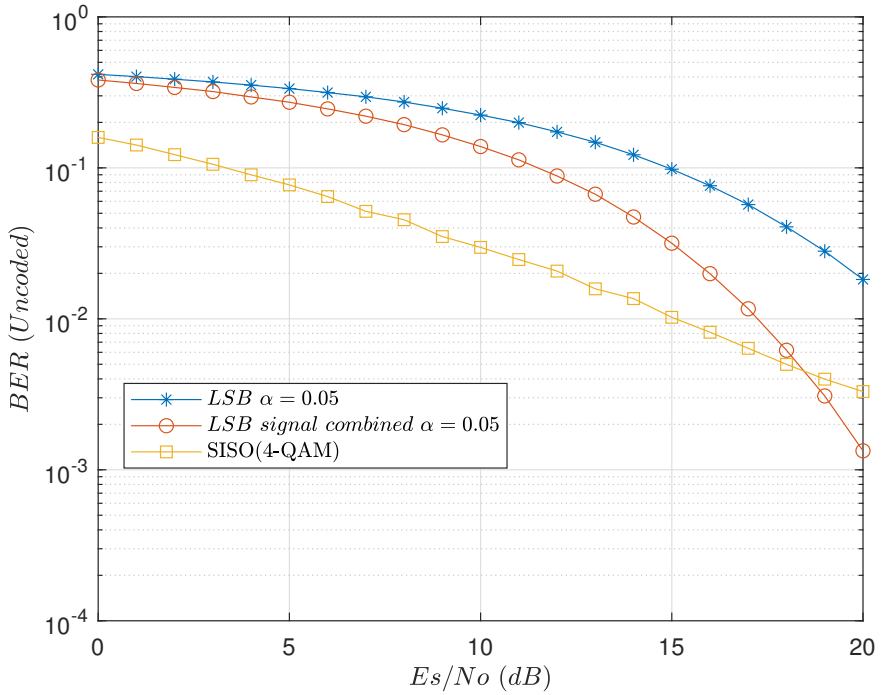

Figure 4.13. Un-coded BER performance for the case of four transmitting antennas with conventional encoded OSTBC and $\alpha = 0.05$.

Figure 4.13 and Figure 4.14 represent the un-coded bit error rate (BER) performance versus $\frac{E_s}{N_0}$ where $N = 4$ and $K = 6$ and conventional encoded OSTBC is used for two different values of $\alpha = 0.05$ and $\alpha = 0.10$, respectively. A reasonable performance gain is attained compared with the first scenario, which is due to the conventional encoded OSTBC when increasing the number of transmitting antennas. Herein, increasing the number of users has no effect on the LSB signal combining since it is performed only between each two successive users.

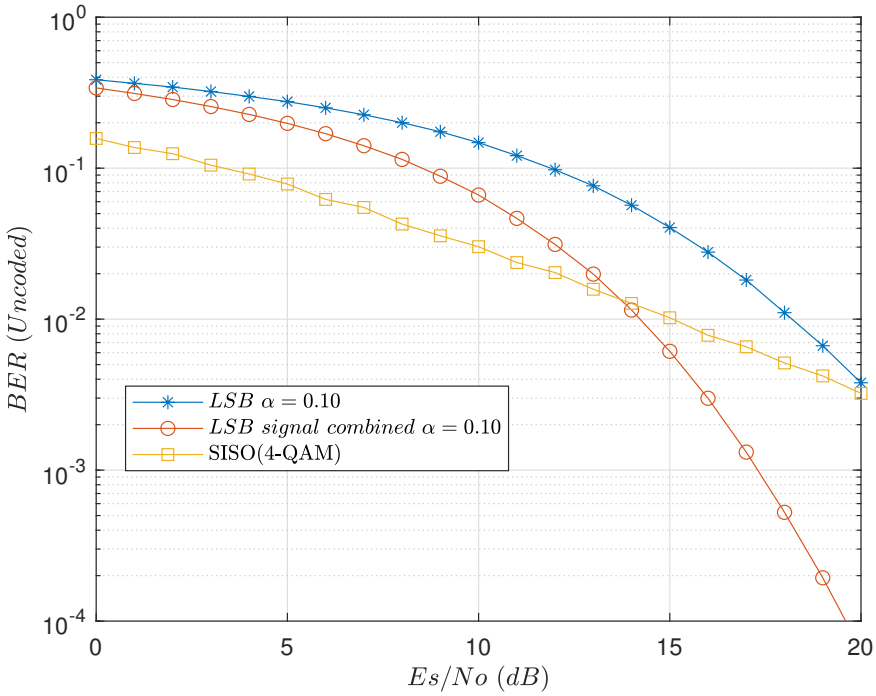

Figure 4.14. Un-coded BER performance for the case of four transmitting antennas with conventional encoded OSTBC and $\alpha = 0.10$.

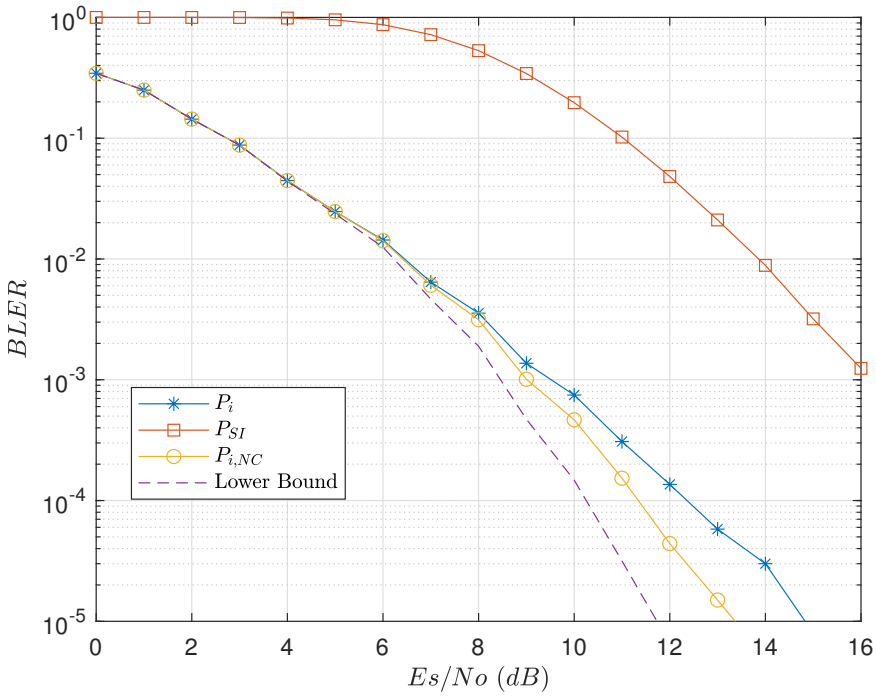

Figure 4.15. BLER performance for the case of four transmitting antennas with conventional encoded OSTBC and $\alpha = 0.05$.

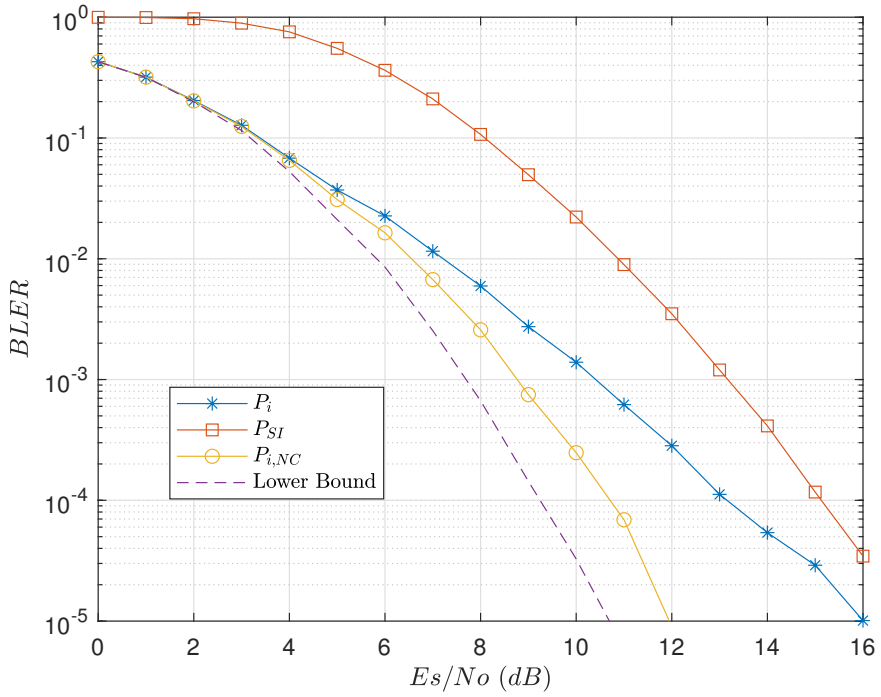

Figure 4.16. BLER performance for the case of four transmitting antennas with conventional encoded OSTBC and $\alpha = 0.10$.

Figure 4.15 and Figure 4.16 illustrate the block error rate (BLER) performance over $\frac{E_s}{N_0}$ for the situation where $N = 4$, $K = 6$ and conventional OSTBC is used for two different values of $\alpha = 0.05$ and $\alpha = 0.10$, respectively. The results provided demonstrate that significant gains can be achieved compared with results shown in Figure 4.11 and Figure 4.12. This is mainly caused by conventional OSTBC when increasing the number of transmitting antennas.

5. CONCLUSION

With the advent of 5G, there has been considerable effort in communications with higher reliability. If one is to consider control applications in an industry setting and to be able to replace wires, a credible demonstration of achieved reliability through wireless is extremely important. One can easily think of factories of future (FoF), autonomous vehicles (AVs), surgeries with robotic equipment controlled from a distant place and so on. All these depend critically on the reliability of the link and its performance.

In this thesis a downlink MU-MIMO scheme to achieve a highly reliable transmission is investigated with the use of a new encoded OSTBC approach where the main benefit is that multiple users can be accommodated with the same resource. Superposition modulation is considered as well to support the SI dissemination so that no extra resources are spent, thus the overall spectral efficiency is not degraded. Furthermore, a constructive combining of LSBs of the received symbols through sub-constellation alignment is employed. Details of the transmitter and receiver processing are well described. Besides, the analytical expressions related with the proposed system model are derived.

The bit error rate (BER) and block error rate (BLER) simulation results for different scenarios depending on the number of transmitting antennas at the base station and consequently the multiple users accommodated by the system show the significant performance gain obtained by the proposed scheme. Enhanced reliability is seen with an increased number of users at the expense of lowering the rate. Another advantage offered by the new encoded OSTBC approach is that multiple users can be accommodated by sharing only a single resource. Due to the higher expected latency with the number of users, simulation results are also shown when conventional OSTBC is utilized where high rate codes are incorporated. A significantly higher reliability is realized at the expense of employing as much as orthogonal resources as the number of users considered. Simulation results also show that the reliability can be further improved in this case by increasing the number of transmit antennas at the base station.

Reliability performance of the proposed downlink MU-MIMO system was analyzed and evaluated. However, as future work latency need to be taken into account in order to get a more practical performance. Furthermore, we aim to study the impact of channel error as the alignment mechanism rely on channel estimates, also the sensitivity of the achievable gain to the correlation of the channel coefficients should be investigated.

A superposition modulation by combining two 4-QAM constellations is considered in this work, higher-order modulation such as 16-QAM, 64-QAM, and 256-QAM are likely to be used to boost the transmission rate.

6. REFERENCES

[1] Dahlman E., Mildh G., Parkvall S., Peisa J., Sachs J., Selén Y. & Sköld J. (2014) 5G wireless access: requirements and realization. IEEE Communications Magazine 52, pp. 42–47.

[2] ITU-R R.I.R.M. (2015), 2083-0: IMT Vision–Framework and Overall Objectives of the Future Development of IMT for 2020 and Beyond.

[3] Vural M., Jung P. & Stanczak S. (2016) On some physical layer design aspects for machine type communication. In: Proceedings of the 20th International ITG Workshop on Smart Antennas (WSA), VDE, pp. 1–8.

[4] Ratasuk R., Prasad A., Li Z., Ghosh A. & Uusitalo M.A. (2015) Recent advancements in M2M communications in 4G networks and evolution towards 5G. In: IEEE 18th International Conference on Intelligence in Next Generation Networks (ICIN), pp. 52–57.

[5] Brahmi N. & Venkatasubramanian V. (2013) Mobile and wireless communications enablers for the twenty-twenty information society (METIS). Tech. Rep. .

[6] Bockelmann C., Pratas N., Nikopour H., Au K., Svensson T., Stefanovic C., Popovski P. & Dekorsy A. (2016) Massive machine-type communications in 5G: Physical and MAC-layer solutions. IEEE Communications Magazine 54, pp. 59–65.

[7] Dawy Z., Saad W., Ghosh A., Andrews J.G. & Yaacoub E. (2017) Toward massive machine type cellular communications. IEEE Wireless Communications 24, pp. 120–128.

[8] Schulz (2017) Latency critical IoT applications in 5G: Perspective on the design of radio interface and network architecture. IEEE Communications Magazine 55, pp. 70–78.

[9] Ji H., Kim Y., Lee J., Onggosanusi E., Nam Y., Zhang J., Lee B. & Shim B. (2017) Overview of full-dimension MIMO in LTE-Advanced Pro. IEEE Communications Magazine 55, pp. 176–184.

[10] Han S., Chih-Lin I., Xu Z. & Rowell C. (2015) Large-scale antenna systems with hybrid analog and digital beamforming for millimeter wave 5G. IEEE Communications Magazine 53, pp. 186–194.

[11] Ji H., Park S., Yeo J., Kim Y., Lee J. & Shim B. (2018) Ultra-reliable and low-latency communications in 5G downlink: Physical layer aspects. IEEE Wireless Communications 25, pp. 124–130.

[12] Popovski P. (2014) Ultra-reliable communication in 5G wireless systems. In: IEEE 1st International Conference on 5G for Ubiquitous Connectivity (5GU), pp. 146–151.

[13] Andrews J.G. (2013) Seven ways that HetNets are a cellular paradigm shift. IEEE Communications Magazine 51, pp. 136–144.

[14] Popovski P. (2018) Wireless access for ultra-reliable low-latency communication: Principles and building blocks. IEEE Network 32, pp. 16–23.

[15] Bennis M., Debbah M. & Poor H.V. (2018) Ultrareliable and low-latency wireless communication: Tail, risk, and scale. Proceedings of the IEEE 106, pp. 1834–1853.

[16] Li C.P., Jiang J., Chen W., Ji T. & Smee J. (2017) 5G ultra-reliable and low-latency systems design. In: IEEE European Conference on Networks and Communications (EuCNC), pp. 1–5.

[17] Konečnỳ J., McMahan H.B., Ramage D. & Richtárik P. (2016) Federated optimization: Distributed machine learning for on-device intelligence. arXiv preprint arXiv:1610.02527 .

[18] Zeydan E., Bastug E., Bennis M., Kader M.A., Karatepe I.A., Er A.S. & Debbah M. (2016) Big data caching for networking: Moving from cloud to edge. IEEE Communications Magazine 54, pp. 36–42.

[19] Baştuğ E., Bennis M. & Debbah M. (2014) Living on the edge: The role of proactive caching in 5G wireless networks. arXiv preprint arXiv:1405.5974 .

[20] López O.L.A., Alves H., Nardelli P.H.J. & Latva-aho M. (2018) Aggregation and resource scheduling in machine-type communication networks: A stochastic geometry approach. IEEE Transactions on Wireless Communications 17, pp. 4750–4765.

[21] López O.L.A., Alves H. & Latva-Aho M. (2018) Rate control under finite blocklength for downlink cellular networks with reliability constraints. In: IEEE 15th International Symposium on Wireless Communication Systems (ISWCS), pp. 1–6.

[22] Benedetto S. & Biglieri E. (1999) Principles of digital transmission: with wireless applications. Springer Science & Business Media.

[23] Ryan W. & Lin S. (2009) Channel codes: classical and modern. Cambridge university press.

[24] Costello D.J. (1983) Error Control Coding: Fundamentals and Applications. prentice Hall.

[25] Anttalainen T. (2003) Introduction to telecommunications network engineering. Artech House.

[26] Ziemer R.E. & Peterson R.L. (2001) Introduction to digital communication. Prentice Hall Upper Saddle River, NJ, second ed.

[27] Sun H., Ng S.X. & Hanzo L. (2012) Superposition coded modulation for cooperative communications. In: IEEE Vehicular Technology Conference (VTC Fall), pp. 1–5.

[28] Ahlswede R., Cai N., Li S.Y. & Yeung R.W. (2000) Network information flow. IEEE Transactions on Information Theory 46, pp. 1204–1216.

[29] Ho T. & Lun D. (2008) Network coding: an introduction. Cambridge University Press.

[30] Li S.Y., Yeung R.W. & Cai N. (2003) Linear network coding. IEEE Transactions on Information Theory 49, pp. 371–381.

[31] Sun Y. & Xiong Z. (2006) Progressive image transmission over space-time coded OFDM-based MIMO systems with adaptive modulation. IEEE Transactions on Mobile Computing 5, pp. 1016–1028.

[32] Tirkkonen O. & Hottinen A. (2002) Square-matrix embeddable space-time block codes for complex signal constellations. IEEE Transactions on Information Theory 48, pp. 384–395.

[33] Tarokh V., Jafarkhani H. & Calderbank A.R. (1999) Space-time block codes from orthogonal designs. IEEE Transactions on Information Theory 45, pp. 1456–1467.

[34] Tarokh V., Jafarkhani H. & Calderbank A. (1998) The application of orthogonal designs to wireless communication. In: IEEE Information Theory Workshop, pp. 46–47.

[35] Duong Q.T. & Tran H.A. (2008) Distributed space-time block codes with amicable orthogonal designs. In: IEEE Radio and Wireless Symposium.

[36] Alamouti S.M. (1998) A simple transmit diversity technique for wireless communications. IEEE Journal on Selected Areas in Communications 16, pp. 1451–1458.

[37] Proakis J.G. & Salehi M. (2001) Digital communications, vol. 4. McGraw-hill New York.

[38] Clarke R. (1968) A statistical theory of mobile-radio reception. Bell system technical journal 47, pp. 957–1000.

[39] Pop M.F. & Beaulieu N.C. (2001) Limitations of sum-of-sinusoids fading channel simulators. IEEE Transactions on Communications 49, pp. 699–708.

[40] Jakes W.C. & Cox D.C. (1994) Microwave mobile communications. Wiley-IEEE Press.

[41] Haghighat A. & Herath S.P. (2017) High Reliability Downlink Transmission with Superposition Modulated Side Information. In: IEEE Wireless Communications and Networking Conference (WCNC), pp. 1–6.

[42] 3GPP RAN1 Meeting#83, TR 36.859 (2015), Study on Downlink Multiuser Superposition Transmission (MUST) for LTE.

[43] Su W., Xia X.G. & Liu K.R. (2004) A systematic design of high-rate complex orthogonal space-time block codes. IEEE Communications Letters 8, pp. 380–382.